

# Snow-Cover Mapping and Monitoring in the Hindu Kush-Himalayas





# Snow-Cover Mapping and Monitoring in the Hindu Kush-Himalayas

Deo Raj Gurung  
Amarnath Giriraj  
Khun San Aung  
Basanta Shrestha  
Anil V Kulkarni

### Published by

International Centre for Integrated Mountain Development  
GPO Box 3226, Kathmandu, Nepal

### Copyright © 2011

International Centre for Integrated Mountain Development (ICIMOD)  
All rights reserved. Published 2011

**ISBN** 978 92 9115 218 6 (printed)

978 92 9115 219 3 (electronic)

**LCCN** 2011-312014

**Photos:** Cover, Birendra Bajracharya; viii, Sanjeev Bhuchar

### Printed and bound in Nepal by

Quality Printers Pvt. Ltd., Kathmandu, Nepal

### Production team

A Beatrice Murray (Consultant editor)

Andrea Perlis (Senior editor)

Dharma R Maharjan (Layout and design)

Asha Kaji Thaku (Editorial assistant)

### Note

This publication may be reproduced in whole or in part and in any form for educational or non-profit purposes without special permission from the copyright holder, provided acknowledgement of the source is made. ICIMOD would appreciate receiving a copy of any publication that uses this publication as a source. No use of this publication may be made for resale or for any other commercial purpose whatsoever without prior permission in writing from ICIMOD.

The views and interpretations in this publication are those of the author(s). They are not attributable to ICIMOD and do not imply the expression of any opinion concerning the legal status of any country, territory, city or area of its authorities, or concerning the delimitation of its frontiers or boundaries, or the endorsement of any product.

This publication is available in electronic form at [www.icimod.org/publications](http://www.icimod.org/publications)

**Citation:** Gurung, DR; Amarnath, G; Khun, SA; Shrestha, B; Kulkarni, AV (eds) (2011) *Snow-cover mapping and monitoring in the Hindu Kush-Himalayas*. Kathmandu: ICIMOD

# Foreword

Snow is an important component of the cryosphere, and the study of snow trends is essential for understanding regional climate change and managing water resources. Changes in the snow budget will have long-term socioeconomic and environmental implications for agriculture, water-based industries, environment, land management, water supplies, and many other development activities. Detailed knowledge about snow cover in space and time is important for assessing water discharge, understanding and mitigating snow disasters, and analysing climate change.

While several institutions and individuals have carried out snow cover studies in the Hindu Kush-Himalayan (HKH) region over the past century, research has been intermittent, unsystematic, and uncoordinated over the long term. The present report provides a summary of a recent systematic mapping and monitoring study of snow cover in the region.

Following the recommendations of a consultation with regional and international partners held in 2008, ICIMOD has established a regional monitoring scheme for snow in the HKH region. The initiative was supported by the Swedish International Development Cooperation Agency (Sida) through a project entitled 'Too Much, Too Little Water – Adaptation Strategies to Climate-Induced Water Stress and Hazards in the Greater Himalayan Region'.

The present report documents the first comprehensive status report of snow cover in the HKH region using decadal (2000–2010) 8-day snow products recorded by moderate resolution imaging spectroradiometer (MODIS). It presents an account of snow mapping and monitoring initiatives at different levels from regional to global. It discusses the role of regional organisations such as ICIMOD, and describes the methodology adopted at ICIMOD for regular monitoring of snow cover. Detailed findings are presented on the status of snow cover in the Hindu Kush-Himalayas overall and in the ten major river basins in the region. Decadal snow cover trends are evaluated based on season, altitude, and region. Both interannual and intra-annual trends are described for different areas (west, central, and east). The snow cover database with interactive mapping application can be accessed through the Mountain Geoportal at <http://geoportal.icimod.org/cryosphere>.

This is the start of a long-term effort. Longer-term data are needed in order to understand the relation between snow cover and climate change. The 10-year snow cover analysis shows regional variations, but the time frame is insufficient to draw significant conclusions. It will also be important to investigate the downstream consequences for the use of the water resources. We hope that the present report, with its detailed account of snow status and trends, together with the snow database, will help bridge the data and information gap on snow cover and support further research initiatives. We also hope that it will provide information that will be useful for planners and policy makers in formulating policies that are relevant for addressing the issues on the ground.

On behalf of ICIMOD, I would like to thank Sida for its generous support. Special appreciation goes to ICIMOD colleagues and the partners who participated in the initial consultation process and helped to formulate the implementation plan which finally resulted in this publication.

**Andreas Schild**  
Director General  
ICIMOD

# Acknowledgements

The team remembers and thanks the late Ms Monica Moktan, the Senior Programme Associate during the early phase of the project. She contributed to the smooth running of the project and its timely completion through her commitment in managing the many administrative details.

This publication was prepared under the ICIMOD project 'Too Much, Too Little Water – Adaptation Strategies to Climate-Induced Water Stress and Hazards in the Greater Himalayan Region' supported by the Swedish International Development Cooperation Agency (Sida). The team is extremely appreciative of the generous support.

Many ICIMOD staff members assisted throughout the project in many different ways. Our thanks go to all of them, in particular to Mr Gauri Dangol for graphic design and Mr Pradeep Dangol for analysis of the data. Various colleagues contributed sections of the report, and we especially thank Mr Rajen Bajracharya and Mr Bikash Dangol of ICIMOD, and Dr Bo-Hui Tang of the Institute of Geographic Sciences and Natural Resources Research (IGSNRR), Chinese Academy of Sciences (CAS), Beijing, for their contributions.

The team is indebted to Dr Andreas Schild, Director General of ICIMOD, for his support and guidance which saw the project through to its completion.

We also thank the ICIMOD publications team, especially Ms Andrea Perlis (Head of Publishing), Ms Greta Rana and Dr A Beatrice Murray (Editorial Consultants), and Mr Dharma Ratna Maharjan and Mr Asha Kaji Thaku for preparation of the final publication.

# Contents

|  |           |
|--|-----------|
| Foreword   | iii       |
| Acknowledgements                                     | iv        |
| Acronyms and Abbreviations                           | vi        |
| Executive Summary                                    | vii       |
| <b>Introduction</b>                                  | <b>1</b>  |
| <b>Snow Cover Mapping and Monitoring Initiatives</b> | <b>2</b>  |
| Global Initiatives                                   | 2         |
| Regional Initiatives – the Hindu Kush-Himalayas      | 3         |
| National Level                                       | 3         |
| <b>Regional Cryosphere Data Hub</b>                  | <b>4</b>  |
| <b>Data Sources</b>                                  | <b>5</b>  |
| Snow Cover Data                                      | 5         |
| Digital Elevation Model (DEM)                        | 6         |
| Boundary Database                                    | 7         |
| <b>Methodology</b>                                   | <b>8</b>  |
| NASA’s Algorithm for Mapping Snow Cover              | 8         |
| Improvement of MODIS Snow Cover Products             | 9         |
| Topographic Variables                                | 11        |
| Estimation of Area                                   | 12        |
| Statistical Significance Test                        | 12        |
| Sensitivity Analysis                                 | 12        |
| Accuracy Assessment and Validation                   | 12        |
| <b>Results of Filtering and Accuracy Assessment</b>  | <b>14</b> |
| Spatial Filtering Window                             | 14        |
| Filtering Process                                    | 14        |
| Accuracy Assessment                                  | 14        |
| <b>Snow Cover Status</b>                             | <b>16</b> |
| Hindu Kush-Himalayan Region                          | 16        |
| Variation in Snow Cover Area                         | 16        |
| The Ten Major River Basins                           | 22        |
| <b>Discussion</b>                                    | <b>28</b> |
| The Snow-Mapping Algorithm                           | 28        |
| Spatial Visualisation and Dissemination System       | 28        |
| Applications   | 28        |
| Hydrological Modelling: A case study                 | 28        |
| <b>Conclusions and Recommendations</b>               | <b>29</b> |
| <b>References</b>                                    | <b>31</b> |

# Acronyms and Abbreviations

|         |  |
|---------|--|
| AVHRR   | Advanced Very High Resolution Radiometer                       |
| AWiFS   | Advanced Wide Field Sensor                                     |
| DEM     | digital elevation model  |
| ENVI    | environmental visual information                               |
| HKH     | Hindu Kush-Himalayas   |
| MODIS   | Moderate Resolution Imaging Spectroradiometer                  |
| MODSPAT | MODIS snow processing and analysis tool                        |
| NASA    | National Aeronautics and Space Administration, United States   |
| NOAA    | National Oceanic and Atmospheric Administration, United States |
| NDSI    | Normalised Difference Snow Index                               |
| NDVI    | Normalised Difference Vegetation Index                         |
| NSIDC   | National Snow and Ice Data Center, United States               |
| RS      | remote sensing   |
| SCA     | snow cover area  |
| Sida    | Swedish International Development Cooperation Agency           |
| SRTM    | Shuttle Radar Topography Mission                               |

# Executive Summary

Snow is an important component of the cryosphere, and an integral part of the global climate system; snow cover both affects and is affected by patterns of climate and climate change. Observation and monitoring of components of the cryosphere are necessary for an understanding of the cryospheric and terrestrial climate system. Predictions about the future state of the environment, in particular the functioning of the climate system, cannot be attempted without thorough analysis of cryospheric processes.

The Hindu Kush-Himalayan (HKH) region contains the greatest expanse of snow and ice outside the polar regions. However, few scientific data are available on snow cover in the region, and the existing data tend to be site specific and short term. The anticipated change in precipitation patterns driven by climate change is likely to have a considerable impact on the more than 1.3 billion people dependent on the Himalayan cryosphere for freshwater. Thus it is increasingly important to develop an overview of snow cover and prepare a basis for assessing future trends.

This report documents the first results of an attempt to develop a comprehensive description of snow cover across the whole HKH region. The study was carried out under the project 'Too Much, Too Little Water – Adaptation Strategies to Climate-Induced Water Stress and Hazards in the Greater Himalayan Region', supported by the Swedish International Development Cooperation Agency (Sida).

Decadal (2000-2010) 8-day snow products recorded by the moderate resolution imaging spectroradiometer (MODIS) were used to analyse the snow cover in the HKH region and the ten major river basins originating from the HKH range. Different filters (temporal, spatial, and altitude-based filters) were used to reduce the influence of cloud pixels in the snow products, particularly for assessment of snow cover area (snow cover area) in absolute figures.

The HKH had 0.76 million sq.km of snow cover area on average, 18.2% of the total land area. Maximum and minimum snow cover area were 1.79 and 0.15 million sq.km (42.9 and 3.6% of the total land area, respectively). The snow cover area was characterised by large inter- and intra-annual variations. The maximum annual average snow cover area was in 2005 and the minimum in 2010. The maximum snow cover was in February and the minimum in July.

Topographic features, such as altitude, aspect, and slope, play a key role in snow distribution. The snow cover area was sensitive to slope at elevations up to 6,000 m; above this, 90% of the area was covered with snow.

The results of snow persistency analyses were not statistically significant, but there was an indication of two peaks with over 90% snow persistency for altitudes above 3,500 m in the winter months, suggesting ablation during summer and accumulation during winter.

Decadal (2000–2010) snow cover area figures for the HKH region were insufficient to yield a statistically significant trend, although there was an indication of an increase in snow cover in the western and eastern HKH region and decrease in the central HKH region.

Among the ten major basins, the Yangtze basin had the greatest area and also the largest mean annual snow cover area (193,304 sq.km, 9.4% of the total land area). Decadal snow cover area trends were not statistically significant, but indicated an increasing trend in some basins and decreasing in others, with seasonal differences. Satellite data such as MODIS snow cover can be very useful for providing estimates that can help compensate for the lack of field-based data. The snow algorithm is being customised for the HKH region, and when finalised will be used to prepare more accurate snow products. These will provide more accurate estimates for use in climate and hydrological modelling. Recommendations are made for future work on snow cover estimation in the HKH region.

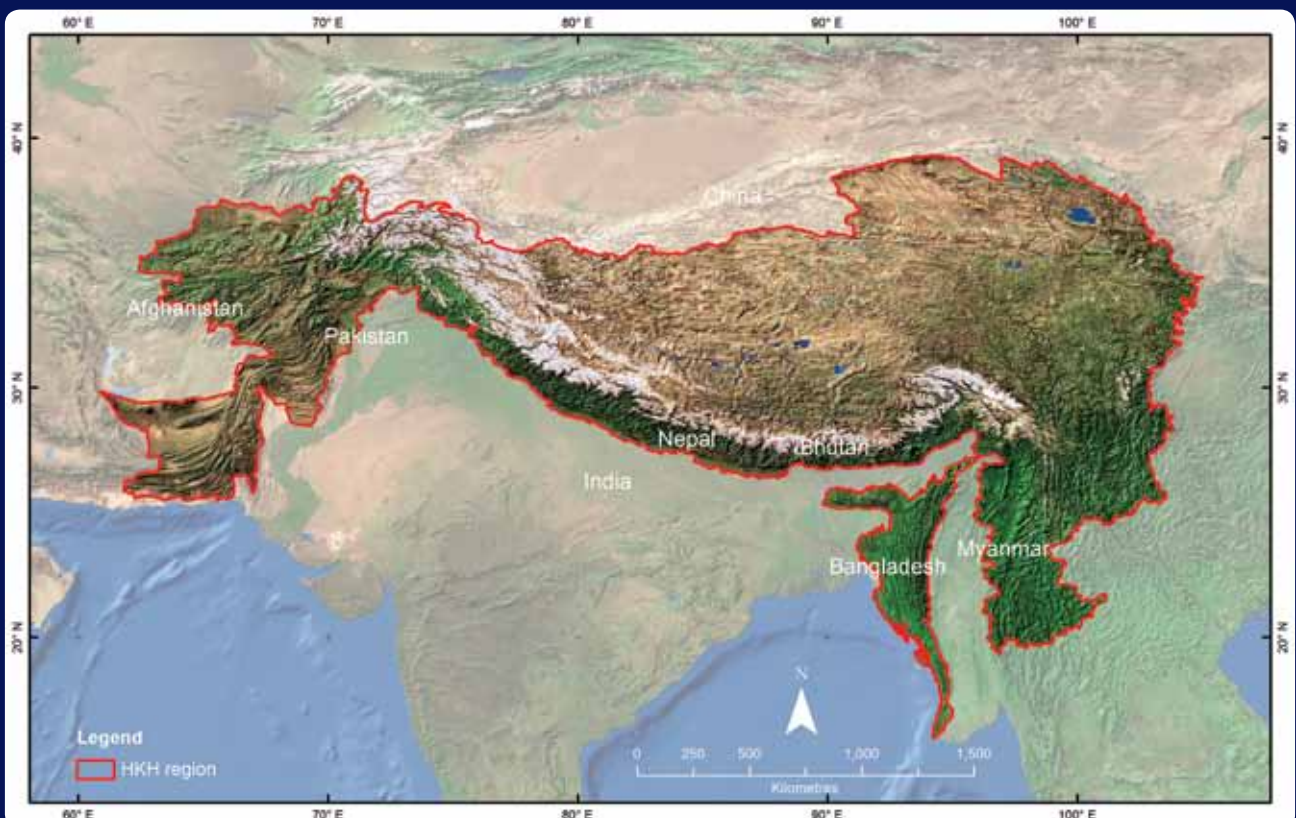


# Introduction

Snow is an important component of the cryosphere – the portion of the Earth’s surface where water is found in solid forms such as ice, glaciers, and permafrost. In the northern hemisphere in winter, about 50% of the land surface is covered with snow. In the Hindu Kush-Himalayas (HKH) (Figure 1), a substantial proportion of the annual precipitation is in the form of snow at high altitudes (above 3,000 m) in both winter and summer. Recently changes have been observed in snowfall patterns with respect to timing, intensity, and duration. The anticipated change in precipitation patterns driven by climate change is likely to have a considerable impact on the more than 1.3 billion people dependent on the Himalayan cryosphere for freshwater.

In the cryosphere, snow is the component that changes most rapidly with the seasons. Because of the feedback effects these changes generate, and their influence on surface energy and atmospheric processes, snow is an important focus for research into climate change and adaptation. The implementation plan of the Global Climate Observation System (GCOS) recognises the areal extent of snow globally as one of the essential climate variables (ECV) for monitoring climate change. Monitoring snow-covered areas and making timely information available on snow cover thus contribute to providing a scientific basis for sound government policies on water use and adaptation to climate change.

**Figure 1: MODIS coverage of the HKH region**



# Snow Cover Mapping and Monitoring Initiatives

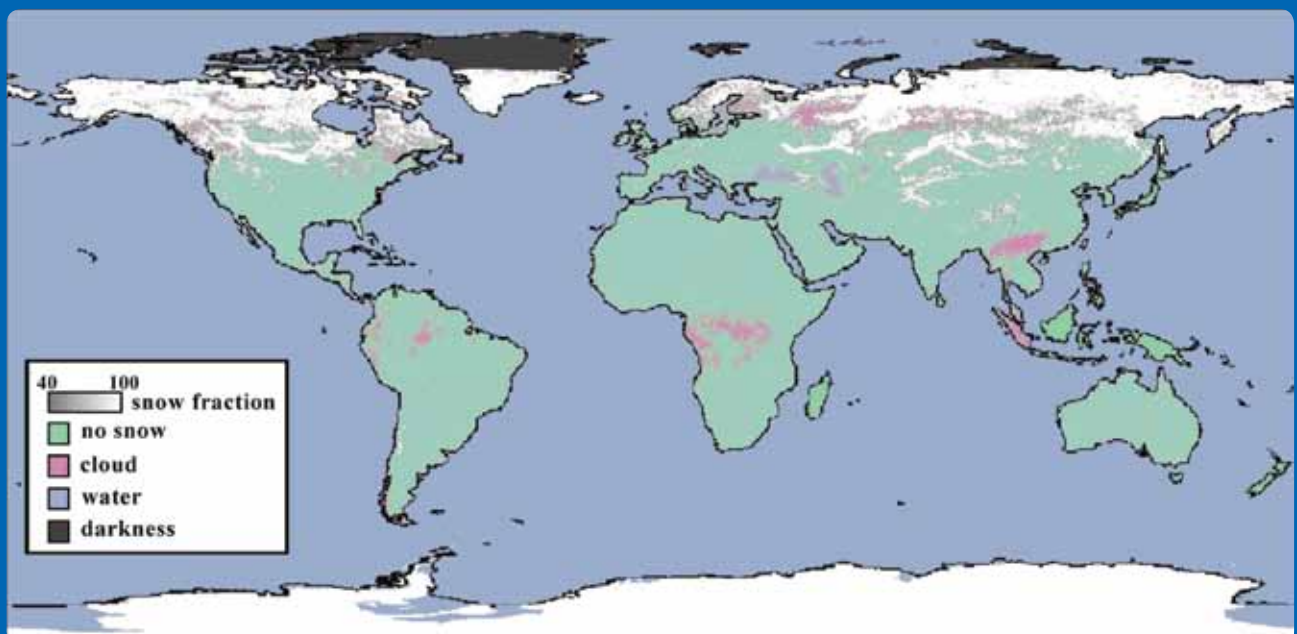
## Global Initiatives

The launch of a weekly analysis chart on snow and ice cover for the northern hemisphere in October 1966 by the Satellite Analysis Branch of the National Oceanic and Atmospheric Administration's (NOAA's) National Environmental Satellite, Data, and Information Service (NESDIS) signalled the inception of long-term snow mapping and monitoring on a continental scale (Hall et al. 2002). The chart uses the visible satellite imagery of the polar operational environmental satellite (POES) and NOAA's geostationary operational environmental satellite (GOES). A weekly snow map of the northern hemisphere was generated from October 1966 to June 2007, at first with a spatial resolution of 180 km, which was improved to reach a spatial resolution of 25 km in mid-1999, using NOAA's interactive multisensory snow and ice mapping system (IMS) (Ramsay 1998), and further to 4 km in February 2004. The Northern Hemisphere EASE-Grid Weekly Snow Cover and Sea Ice Extent database was the first long-term database for these environmental variables (Robinson et al. 1993). The database is archived and distributed through the server of the National Snow and Ice Data Centre (NSIDC).

Improved mapping of snow cover area (SCA) started with the launch on 18 December 1999 and 4 May 2002, respectively, of the Terra and Aqua satellites with moderate resolution imaging spectroradiometers (MODIS) by the National Aeronautics and Space Administration (NASA) (Figure 2). These provided snow cover products with a resolution of 500 m. Daily snow maps from Terra and Aqua are produced by NASA's Goddard Space Flight Centre (GSFC) and have been available since February 2000 and August 2002, respectively.

The launch of a Meteosat second generation satellite (MSG-1) in 2002 by European organisations enabled generation of daily snow cover maps over Europe from January 2005.

**Figure 2: Eight-day composite global MODIS snow-cover map for 24–31 October 2001**



Source: Hall et al. (2002)

## Regional Initiatives – the Hindu Kush-Himalayas

To date, there has been no coordinated regional monitoring initiative to monitor snow regularly in the HKH region. A regional consultative workshop on 'Remote Sensing of the Cryosphere' convened by ICIMOD in early 2009 revealed that India and China are ahead of other countries in the region in terms of snow mapping and monitoring (ICIMOD 2009). Monitoring, however, is either site specific and confined to catchments or basins during months when snowfall is high, mainly for flood forecasting, or confined to a local network of stations in certain parts of the region. There is no regional mapping and monitoring perspective and no coordination among institutions across the region to adopt a regional framework to address the data gap. The need for a framework for a Himalayan snow cover information system (HIMSIS) was expressed as long ago as 1991 (Ramamoorthi and Haefner 1991).

## National Level

India began snow mapping in 1976 in the then National Remote Sensing Agency (NRSA). SCA mapping was carried out for the Sutlej basin using the NOAA's advanced very high resolution radiometer (AVHRR), and this was later extended to the Beas basin (Ramamoorthi and Haefner 1991). Many mapping exercises have been carried out in the recent past using Indian Remote Sensing Satellite (IRS) data, but systematic monitoring of seasonal SCA using advanced wide field sensor (AWiFS) data only began after the launch of the Resourcesat satellite in 2004. Snow cover for 28 sub-basins was estimated in the western and central Himalayas and for three basins in the eastern Himalayas for a period from October to June for four years commencing in 2004 (Kulkarni et al. 2010; Kulkarni et al. 2008). Snow extent was estimated at intervals of 5 or 10 days, depending upon the AWiFS data available. Other studies confined to specific sites, basins, or watersheds have also been carried out recently (Kulkarni et al. 2002; Krishna 2005; Kaur et al. 2009; Negi et al. 2009; Rathore et al. 2009).

Ground-based snow monitoring has been carried out in eastern China since the late 1800s (Brown 2000), while data for western China have been available since 1951 (Dahe et al. 2006). Monitoring snow cover in China using remote sensing started only in the early 1990s (Zhang et al. 2010). There is no system operational as yet for regular monitoring of snow using indigenous satellite sensors. Many recent studies (Dahe et al. 2006; Liang et al. 2007; Li et al. 2008; Pu and Xu 2009) on spatio-temporal variability of snow cover are still based on global datasets such as MODIS, scanning multichannel microwave radiometer (SMMR), and the special sensor microwave/imager (SSM/I).

Pakistan and Bangladesh are fairly new players in the field of space science and applications. National space programmes such as the Pakistan Space and Upper Atmosphere Research Commission (SUPARCO) and Bangladesh Space Research and Remote Sensing Organisation (SPARRSO) are currently consolidating their capacities.

The remaining HKH countries of Afghanistan, Bhutan, Myanmar, and Nepal do not have national space programmes. In these countries, much depends on external projects. A typical case is the Agromet Project, which maps and monitors snow extent in Afghanistan using MODIS snow products and distributes information through a monthly bulletin.

# Regional Cryosphere Data Hub

A regional consultative workshop held in 2009 (ICIMOD 2009) recommended establishing a regional cryosphere data hub to address the data gap through consolidation of national efforts and adopting a common framework. The International Centre for Integrated Mountain Development (ICIMOD), as a regional organisation working for sustainable development of the HKH region, was suggested for the role.

ICIMOD began efforts to establish a regional cryosphere hub supported by the Swedish International Development Cooperation Agency (Sida) through a project entitled 'Too Much, Too Little Water'. The project aimed to strengthen resilience among mountain people and downstream populations to withstand, and adapt to, climate change induced constraints and hazards related to water. One part of the project focused on possible future changes in water availability. Snow is an important factor. Storage of precipitation in the form of snow and subsequent slow release of snowmelt plays an important role in the supply of water for agriculture and consumption in much of the region. As there was no comprehensive assessment available of SCA in the region, or of changes in the pattern of SCA over time, the project designed a methodology for snow cover mapping in the HKH region using remote sensing techniques – the only feasible option for achieving wide-scale coverage in this poorly accessible and thinly populated area. This publication describes the methodology that was implemented and the first results of this work.

Access to data remains a challenge in this part of the region. Stringent policies regulate data sharing, and there is no infrastructure to facilitate it. A portal dedicated to the cryosphere will provide a single gateway to the snow data generated, from the end of 2011.

ICIMOD introduced geographical information system (GIS) and remote sensing (RS) technologies in the early 1990s, establishing a dedicated division (the Mountain Environment and Natural Resources Information system [MENRIS]). Over time MENRIS has become a centre for geo-informatics, capacity-building, and developing applications. In the late 1990s, ICIMOD developed an inventory of glaciers and glacial lakes at regional level for the HKH based on remote sensing and other maps and images; the results were published from 2001 onwards (Mool et al. 2001a; 2001b, Ives et al. 2010). Mapping and monitoring of snow is a new activity added only recently. Snow mapping is data intensive: temporal variability means that detailed data need to be collected throughout the year, at the same time, the changes over short distances and with small changes in altitude can only be captured at medium to high spatial resolution. Snow monitoring takes place in a daily and/or weekly time frame using medium resolution satellite data and requires a special expertise not widely available in the region.

# Data Sources

## Snow Cover Data

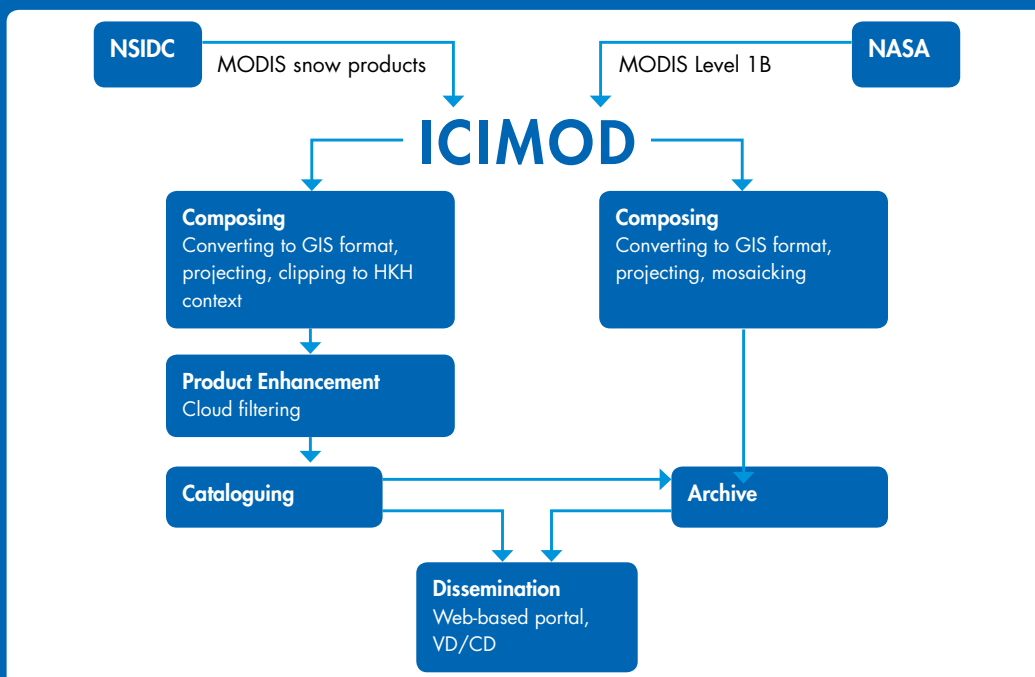
Daily MODIS snow products at 500 m spatial resolution were used for snow mapping and monitoring. The system implemented at ICIMOD to generate enhanced 8-day snow cover products used global MODIS snow products accessed through subscription arrangements made with the National Snow and Ice Data Centre (NSIDC), Boulder, USA. The approach is summarised in Figure 3. A package of MODIS snow products (Table 1) has been created by the Goddard Space Flight Centre (GSFC) from automated algorithms as a sequence of products beginning with a swath (scene) and progressing through spatial and temporal transformations to a monthly global snow product

**Table 1: Different types of global snow products based on MODIS sensors**

| Earth science data type (ESDT) | Product level | Nominal data array dimensions | Spatial resolution | Temporal resolution               | Map projection               |
|--------------------------------|---------------|-------------------------------|--------------------|-----------------------------------|------------------------------|
| MOD10_L2                       | L2            | 1,354 km by 2,000 km          | 500 m              | swath (scene)                     | none (lat, long. referenced) |
| MOD10L2G                       | L2G           | 1,200 km by 1,200 km          | 500 m              | day of multiple coincident swaths | sinusoidal                   |
| MOD10A1                        | L3            | 1,200 km by 1,200 km          | 500 m              | day                               | sinusoidal                   |
| MOD10A2                        | L3            | 1,200 km by 1,200 km          | 500 m              | 8 days                            | sinusoidal                   |
| MOD10C1                        | L3            | 360° by 180° (global)         | 0.05° by 0.05°     | day                               | geographic                   |
| MOD10C2                        | L3            | 360° by 180° (global)         | 0.05° by 0.05°     | 8 days                            | geographic                   |

Source: Riggs et al. 2006

**Figure 3: ICIMOD system for generating 8-day snow-cover products for the Hindu Kush-Himalayan region from global MODIS products**



(Riggs et al. 2006). The one currently in use is the 8-Day L3 global 500 m grid, an 8-day composite product from both Terra (MOD10A2) and Aqua (MYD10A2) sensors with morning and afternoon overpasses respectively. There are two types of information, fractional snow cover and maximum snow extent. ICIMOD uses the information on maximum snow extent. This gives the total maximum area of snow cover over 8 days and is generated by stacking 8 days of daily snow maps together. The grid data are available in sinusoidal map projections and in the hierarchical data format-earth observation system (HDF-EOS), a standard archive format for products from the EOS data information system (EOSDIS).

In total 25 tiles of 1,200 by 1,200 km (10°x10°) are required to cover the entire HKH region and all ten major downstream river basins (Figure 4); these are downloaded by NSIDC to the file transfer protocol (FTP) server maintained at ICIMOD. (More information is available at <http://nsidc.org/data/modis/>)

### Digital Elevation Model (DEM)

NASA's shuttle radar topography mission (SRTM) obtained elevation data on a near-global scale and represents the most complete high-resolution digital topographic database on the Earth. The SRTM is a specially modified radar system that flew on board the Space Shuttle Endeavour during an 11-day mission in February 2000. SRTM version 4, the latest in a series of releases, represents a significant improvement from previous versions and uses new interpolation algorithms and improved auxiliary DEMs. The SRTM 90 m DEM for the entire world has been built in a mosaic of seamless near-global coverage (up to 60 degrees north and south) and can be downloaded as 5 x 5 degree tiles in the geographic coordinate system of the World Geodetic System – WGS84 Datum.

Sixty-eight tiles covering the entire HKH region and the ten major downstream river basins were downloaded from the Consultative Group on Agricultural Research-Consortium for Spatial Information (CGIAR-CSI) GeoPortal (<http://srtm.csi.cgiar.org/Index.asp>).

**Figure 4: The 25 tiles of 8-day MODIS snow products covering the HKH region and all ten major river basins; the yellow polygon defines the HKH region**

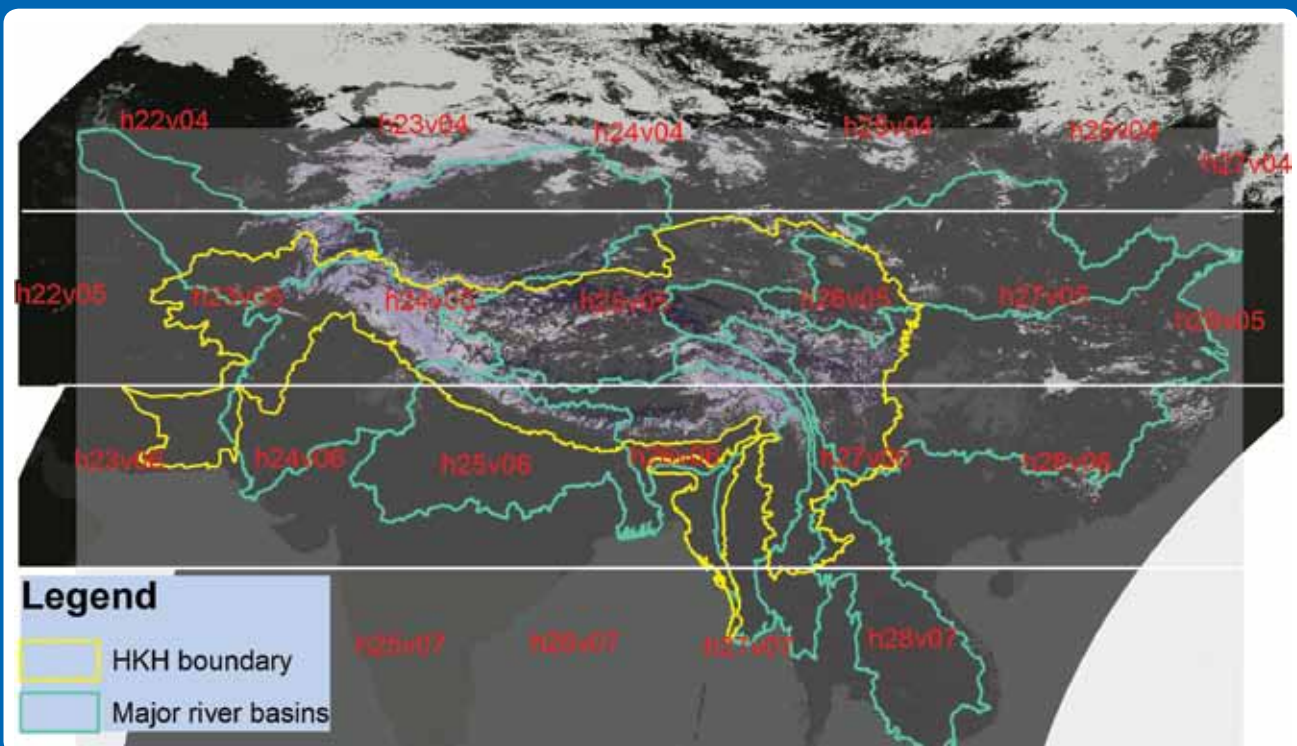
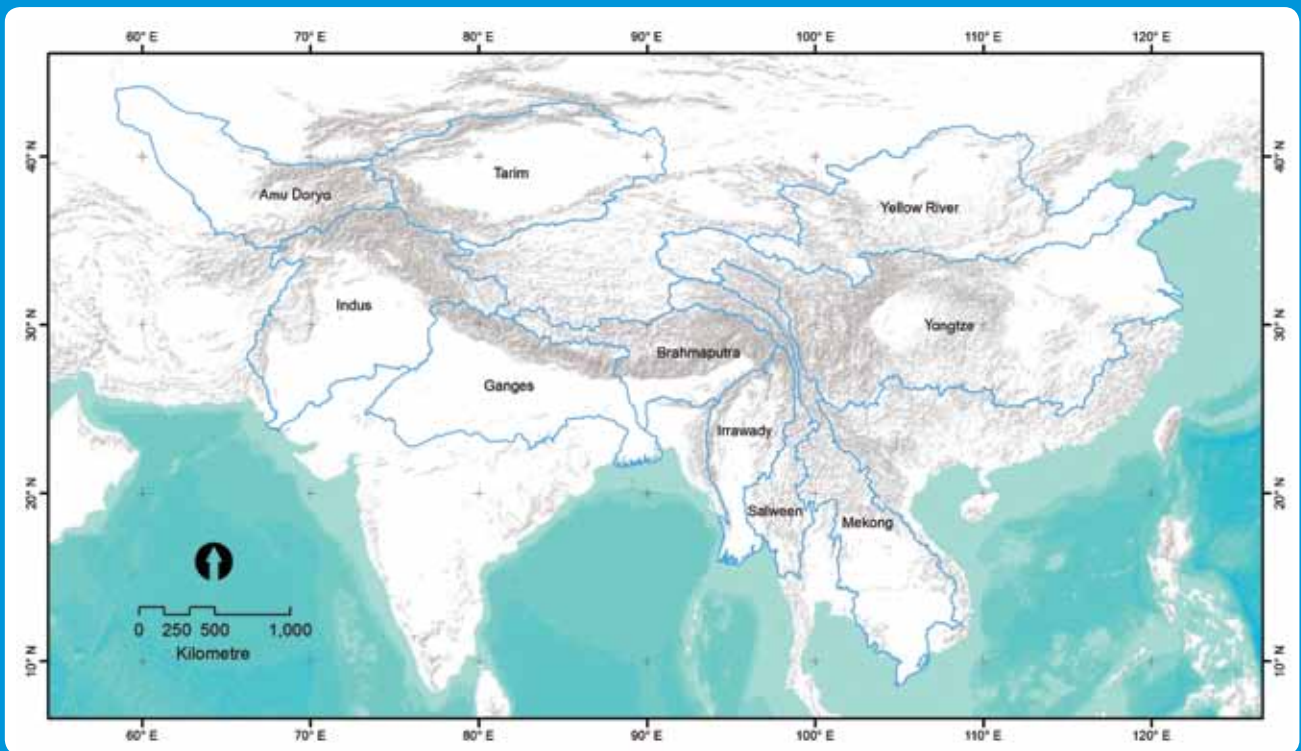


Figure 5: Map of ten major downstream river basins showing their origins in the HKH region



## Boundary Database

Snow cover statistics were derived at two levels: for the ten major river basins (Figure 5), and for the HKH region. The HKH boundary in the ICIMOD database was used to define the HKH region. As no comprehensive basin database was available, one was generated from 90 m SRTM using an Arc Hydro tool in ArcGIS 9.3. It was corroborated using a watershed boundary database generated from different sources, including the Environmental Systems Research Institute (ESRI) database. For entering topology, polylines were edited and basin polygons generated using the Integrated Land and Water Information System (ILWIS) version 3.6.01 software.

# Methodology

## NASA's Algorithm for Mapping Snow Cover

The automated MODIS algorithm for mapping snow cover, Snowmap (Hall et al. 2002), uses satellite reflectance in MODIS bands 4 (0.545–0.565  $\mu\text{m}$ ) and 6 (1.628–1.652  $\mu\text{m}$ ) to calculate the normalised difference snow index (NDSI). The NDSI is a measurement of the relative magnitude of the characteristic reflectance difference between the visible and short-wave infrared (IR) reflectance of snow.

Pixels with approximately 50% or more snow cover have normalised snow difference indices (NDSIs) of 0.4. Since water also has an NDSI of 0.4, a pixel with a band 2 reflectance greater than 11% is mapped as a snow pixel. Should the reflectance of band 4 be less than 10%, however, the pixel will not be mapped as snow even if the other criteria are met. This prevents pixels containing very dark targets, such as black spruce forests, from being mapped as snow (Hall et al. 2002). The normalised difference vegetation index (NDVI) and NDSI are used together to improve snow mapping in dense forests. The NDVI is calculated using MODIS bands 1 (0.620–0.670  $\mu\text{m}$ ) and 2 (0.841–0.876  $\mu\text{m}$ ) as snow will tend to lower the NDVI. If the NDVI =  $\sim 0.1$ , the pixel may be mapped as snow even if the NDSI is  $< 0.4$ .

Distinguishing cloud from snow is a major challenge (Ackerman et al. 1998) and can lead to identification of spurious snow cover (Hall et al. 2002). Although the NDSI can separate snow from most obscuring or heavy clouds, it does not always identify or discriminate clouds that are optically thin or light. To address the cloud issue, a thermal mask was applied using MODIS infrared bands 31 (10.78–11.28  $\mu\text{m}$ ) and 32 (11.77–12.27  $\mu\text{m}$ ). A split-window technique was used to estimate ground temperature; if the temperature of a pixel is  $> 277$  K the pixel will not be mapped as snow.

## Improvement of MODIS Snow Cover Products

There are certain limitations with regard to using RS for mapping of geophysical parameters, thus field-based data is integrated to improve the RS products. Cloud cover and spectral overlap are major issues in mapping of snow cover using RS techniques.

Cloud cover is a particular challenge to optical RS in the HKH region, where skies remain overcast for much of the year. The presence of cloud pixels in MODIS snow cover products is significant during the monsoon season, and leads to an underestimation of SCA, which in turn influences application products such as hydrographs. Methodologies are available to filter out cloud pixels from MODIS snow products (Riggs and Hall 2002; Miller and Thomas 2005; Gafurov and Bardossy 2009).

Misclassification due to spectral overlap is also observed while mapping snow cover using MODIS sensors in the region. The obvious evidence of misclassification is the presence of snow pixels in MODIS snow products in the low-lying belt of the HKH region in a tropical climatic setting.

$$\text{NDSI} = \frac{\text{Band 4} - \text{Band 6}}{\text{Band 4} + \text{Band 6}} \quad (1)$$

The four steps and integrated approach used to reduce misclassification are described in the following.

## Combined Terra and Aqua

Aqua and Terra satellites pass over the equator with a time lag of about three hours, as a result of which there is a good chance of a pixel being cloud free in one of the two. The combination of Terra and Aqua snow products takes place in such a way that a cloud pixel in any one product is replaced by the same (cloud free) pixel from the

other product (Figure 6). This filtering approach was introduced in August 2002 after Aqua snow products became available. The approach has been discussed by Gafurov and Bardossy (2009) and Wang and Xie (2009).

Mathematically the process is expressed by

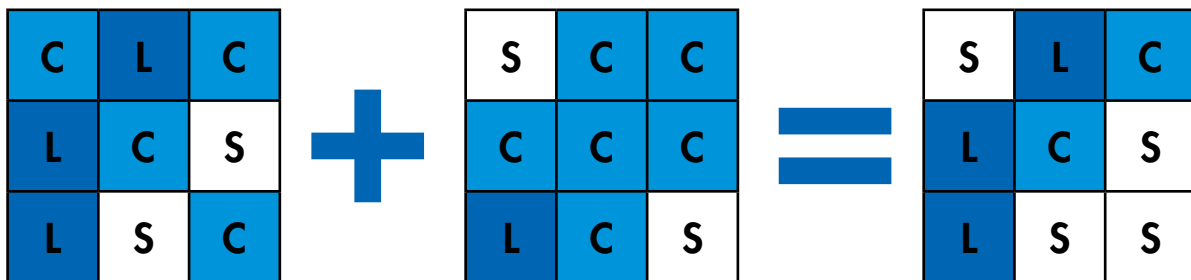
$$S(x, y, t) = \max(S^A(x, y, t), S^T(x, y, t)) \quad (2)$$

where  $y$  is the index for the row (vertical);  $x$  is the index for the column (horizontal);  $t$  is the index for the day (temporal) the pixel  $S$  was mapped, and  $S^A$  and  $S^T$  stand for the Aqua and Terra pixels.

### Temporal filter

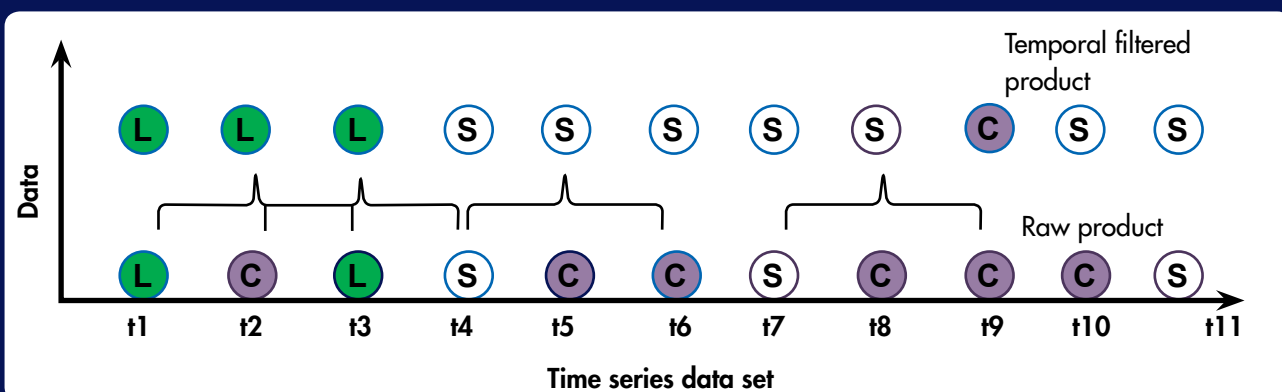
The temporal filter compares three consecutive sets of a combination of products mapped over 8 days (merged Terra and Aqua). Depending on cloud cover mapped in backward and forward products, information is used to fill cloud pixels in the third set of combination snow products. If the backward and forward combinations have the same classes, the corresponding cloud pixel in the third combination is assigned the same class (Figure 7). Otherwise, the backward (earlier) information is considered first and the forward (later) information second. Those pixels under cloud cover in all three sets will be retained as cloud. Figure 7 illustrates how the temporal filter works.

Figure 6: Schematic diagram illustrating cloud filtering by combining Terra and Aqua snow products



C, L and S denote cloud, land, and snow pixels respectively.

Figure 7: Schematic diagram illustrating cloud filtering using the temporal filter



C, L, and S denote cloud, land, and snow pixels respectively.

The filtering process is expressed as follows:

$$S(x, y, t) = 1 \text{ if } (S(x, y, t - 8) = 1 \text{ or } S(x, y, t + 8) = 1) \quad (3)$$

where S-8, S and S+8 are three consecutive combinations of products mapped over 8 days, 1 corresponds to snow cover, and 0 to land cover.

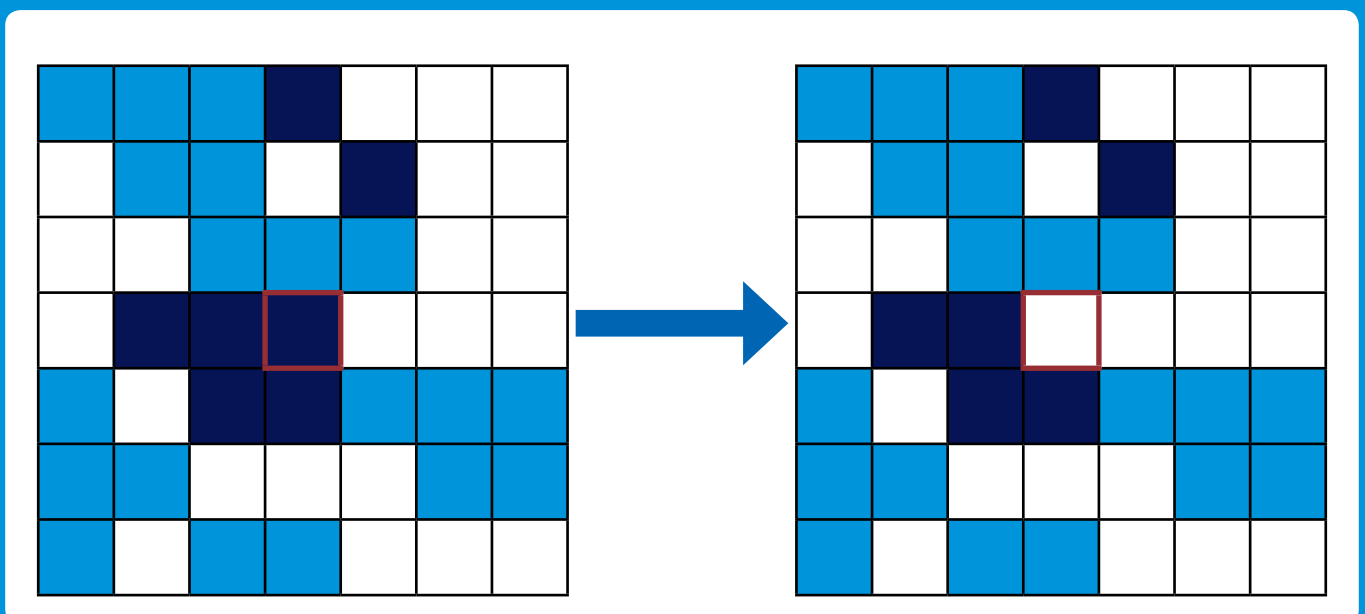
### Spatial filter

The spatial filter works on the basis of a majority algorithm and determines the new value of the cell based on the most popular values within the filter window. The assumption is not always correct, but the probability of a pixel having the same cover as the cover with maximum presence is high. Spatial filtering is applied selectively only to the cloud pixel and missing data, while the rest of the original data are maintained. A 7 x 7 pixel window was chosen because its performance is better than that of other pixel windows. The approach is shown in Figure 8.

### Altitude-based masking

Spectral overlap from different land-cover classes as a result of illumination results in misclassification of non-snow land cover as snow, and as a result scattered snow pixels are observed even in tropical settings. Some pixels in central India were mapped erroneously as snow pixels and had to be corrected. There are limitations to addressing this problem at product level. Masking based on altitude seems to be the only way to deal with scattered snow pixels found at low altitudes. The challenge to implementing altitude-based masking throughout the region lies in assigning the optimum threshold altitude. The snow line varies throughout the HKH, thus there is no valid single threshold value. In total, eight zones were delineated based on references (Jain et al. 2009; Kulkarni et al. 2010), personal communication, and assessment based on mapping of a season of heavy snowfall. Different threshold values were used for all eight zones and snow pixels below threshold altitude were reclassified to surrounding land classes.

**Figure 8: Spatial filtering (7x7 filter window) uses a major class algorithm to eliminate cloud pixels at the centre of the matrix**



## Integrated MODIS snow processing and analysis tool

An integrated MODIS snow processing and analysis tool (MODSPAT) was developed to automate processing and carry out the cloud-filtering processes mentioned above. This tool can also extract snow cover statistics based on characteristics of the terrain (slope, aspect, and altitude).

The core programme was written in C using free and open source libraries for images that are distributed under General Public License. A graphic user interface (Figure 9) was written in Microsoft Visual C# 2008 using Microsoft Visual Studio 2008.

## Topographic Variables

### Altitude map

The SRTM DEM was re-sampled from a spatial resolution of 90 to 500 m using a weighted average algorithm. The new value of a cell was based on a weighted distance average of the input cell. Elevation plays a decisive role in snow accumulation (Jain et al. 2009); the analysis of the distribution and depletion of snow was based on elevation, and the statistics on SCA were generated and analysed based on altitude.

### Aspect map

An aspect map was derived from the re-sampled SRTM DEM. The parameters were calculated by fitting a quadratic surface to the digital elevation data for the kernel size entered and taking the appropriate derivatives using environmental visual information (ENVI) software with a kernel size of 3 x 3. Snow distribution was analysed for 16 aspect classes (Table 2).

### Slope map

A slope map was generated from the re-sampled 500 m SRTM DEM using the topographic modelling module of the ENVI image processing software. The slope was measured in degrees with the convention of 0° for a horizontal plane. For the purpose of altitude-based snow distribution and depletion analysis, slope zones were generated at 15-degree intervals.

**Figure 9: Interface of the tool developed to automate MODIS snow product processing and analysis**

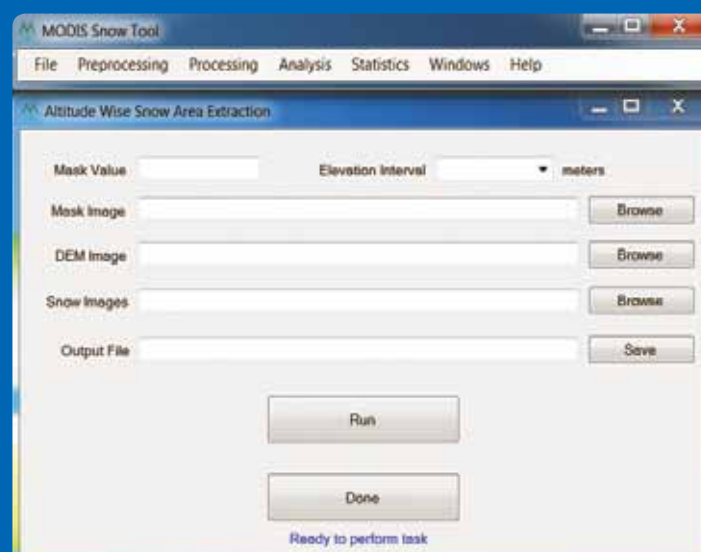


**Table 2: Aspect classes used to analyse snow distribution**

| Range (degrees) | Mid-point (degrees) | Aspect | Range (degrees) | Mid-point (degrees) | Aspect |
|-----------------|---------------------|--------|-----------------|---------------------|--------|
| 348.75–11.25    | 0                   | N      | 168.75–191.25   | 180                 | S      |
| 11.25–33.75     | 22.5                | NNE    | 191.25–213.75   | 202.5               | SSW    |
| 33.75–56.25     | 45                  | NE     | 213.75–236.25   | 225                 | SW     |
| 56.25–78.75     | 67.5                | ENE    | 236.25–258.75   | 247.5               | WSW    |
| 78.75–101.25    | 90                  | E      | 258.75–281.25   | 270                 | W      |
| 101.25–123.75   | 112.5               | ESE    | 281.25–303.75   | 292.5               | WNW    |
| 123.75–146.25   | 135                 | SE     | 303.75–326.25   | 315                 | NW     |
| 146.25–168.75   | 157.5               | SSE    | 326.25–348.75   | 337.5               | NNW    |

## Estimation of Area

The SCA was estimated from the improved MODIS snow product available at 500 m spatial resolution. The products were projected to Albers Equal Area Conic projection to make them consistent with the standard projection system. The projection parameters adopted for the HKH region are given in Table 3.

The areas of the ten major river basins calculated using Albers Equal Area and UTM are shown in Table 4.

## Statistical Significance Test

Trend estimation is a statistical technique to aid interpretation of data; when a series of measurements of a process are treated as a time series, trend estimation can be used to make and justify statements about tendencies in the data. However, a mathematical trend represented by a straight line does not necessarily represent a real trend or reflect the real relationship of the two variables. It is thus important to determine if a measured trend is statistically significant. The statistical significance of a result is the degree to which the result is unlikely to have occurred by chance, or in other words reflects something likely to be 'real'.

In the present study, linear regression was used for trend analysis of SCA and the significance was estimated on the basis of the root mean square error. Values lying within the root mean square error were considered to be statistically significant.

## Sensitivity Analysis

Sensitivity analysis was carried out to assess the performance of different filters in filtering out cloud pixels. SCA and cloud cover area were plotted for the entire HKH region after every filtering step. The statistics on SCA and cloud cover thus obtained were converted to percentages and plotted against time.

## Accuracy Assessment and Validation

Two levels of accuracy assessment were carried out to assess the improvements in the snow cover products.

### Absolute assessment

The method used for absolute accuracy assessment was based on the error matrix. This method enables two sources of spatial information to be compared quantitatively using a common, non-site specific, accuracy assessment method (i.e., only the total amount of each class/category is measured irrespective of its location). This is carried out by superimposing information from the ground station (snow or non-snow) on to a classified image (8-day enhanced MODIS snow product) and comparing the agreement between the information from the classified image and reference points. Overall accuracy and Kappa statistics were estimated using the error matrix thus generated. Overall accuracy – the total agreement and/or disagreement between the maps – was computed by dividing the total

**Table 3: Projection parameters for Albers Equal Area Conic Projection for the HKH region**

| Parameter                   | Name/value              |
|-----------------------------|-------------------------|
| Reference Projection        | Albers Equal Area Conic |
| False Easting               | 0.0                     |
| False Northing              | 0.0                     |
| Central Meridian            | 83.0                    |
| Standard Parallel 1         | 20.0                    |
| Standard Parallel 2         | 36.0                    |
| Latitude of Origin          | 15.0                    |
| Unit                        | metre                   |
| Datum World Geodetic System | 1984                    |
| Spheroid semi-major axis    | 6,378,137.0 m           |
| Spheroid semi-minor axis    | 6,356,752.314 245       |

**Table 4: Areas of the ten major river basins calculated using Albers Equal Area Conic projection and UTM**

| Basin        | Area (sq.km) |           | Difference (UTM-Albers) |        |
|--------------|--------------|-----------|-------------------------|--------|
|              | UTM          | Albers    | sq.km                   | %      |
| Amu Darya    | 645,726      | 645,895   | 169                     | 0.026  |
| Indus        | 1,116,086    | 1,116,347 | 261                     | 0.023  |
| Ganga        | 1,001,019    | 1,001,087 | 68                      | 0.007  |
| Brahmaputra  | 529,447      | 529,449   | 2                       | 0.000  |
| Irrawaddy    | 426,501      | 426,393   | -108                    | -0.025 |
| Salween      | 363,778      | 363,898   | 120                     | 0.033  |
| Mekong       | 841,322      | 841,337   | 15                      | 0.002  |
| Yangtse      | 2,065,763    | 2,066,050 | 288                     | 0.014  |
| Yellow River | 1,073,168    | 1,073,443 | 276                     | 0.026  |
| Tarim        | 929,003      | 929,254   | 252                     | 0.027  |

number of correct sample units by the total number of sample units in the error matrix Kappa statistics, which is a measurement of proportionate reduction in error generated by a classification process compared with the error of a completely random classification.

$$\text{Overall accuracy} = D / N \times 100 \% \quad (4)$$

where  $D$  denotes the total number of correct cells along the major diagonal and  $N$  the total number of cells in the error matrix.

$$\text{Kappa coefficient} = \frac{\sum_{i=1}^r x_{ii} - \sum_{i=1}^r (x_{i+} \times x_{+i}) / N^2 - \sum_{i=1}^r (x_{i+} \times x_{+i})}{N^2 - \sum_{i=1}^r (x_{i+} \times x_{+i})} \quad (5)$$

Where  $r$  is the number of rows in the matrix,  $x_{ii}$  is the total number of correct cells in a class (i.e., value in row  $i$  and column  $i$ ),  $x_{i+}$  is the total for row  $i$ ,  $x_{+i}$  is the total for column  $i$ , and  $N$  is the total number of cells in the error matrix.

The error matrix was implemented in Erdas Imagine 9.2.

### Relative assessment

It is general practice in remote sensing to validate coarser products with finer products using high resolution images and products. This is known as relative assessment, since it is based on relative reference images. Relative assessment of the enhanced MODIS product was carried out using snow cover maps generated from AWiFS. Two sets of AWiFS images captured on 16 and 21 January 2006 were re-sampled from 56 to 500 m to achieve consistency with the enhanced MODIS product. Snow cover was generated using the snow algorithm (Kulkarni et al. 2006) and combined to construct a 5-day composite product using Model Maker in Erdas Imagine 9.3. Both composite snow products (AWiFS and MODIS) were reclassified into two classes (snow and snow free) and assigned consistent codes.

Overall accuracy and Kappa statistics were estimated based on the error matrix using random points (100 points) generated from the enhanced MODIS product and in reference to AWiFS's 5-day composite snow product.

# Results of Filtering and Accuracy Assessment

## Spatial Filtering Window

Spatial filtering was used to filter out undesired cloud and snow classes by running a scan in an optimal window size and reclassifying to the desired class based on different algorithms, including the majority count. Different scan window sizes were used; performance was assessed to arrive at the optimal window size. In the present context, filtering was found to be optimum with a 7 x 7 scan window (Figure 10), thus a 7 x 7 scan window was used in the product enhancement process.

## Filtering Process

Different filters were used to filter out cloud pixels from snow products. Cloud contamination is most prevalent in June, July, and August, with almost a quarter of the region being under cloud cover at the maximum. Figure 11 shows the cloud cover area in the products over a year and the change in cloud cover area after application of different filters. Figure 12 shows the corresponding SCA over the year in the original products and after applying the different cloud cover filters. Overall there was more cloud cover in the Aqua product, which means the region is overcast more in the afternoon than in the morning. Combining Terra and Aqua removed up to 40% of the cloud pixels. Temporal filtering removed up to 50% of the cloud pixels, yielding the best results. Spatial filtering was not as efficient at removing cloud pixels (~5%), but was an important filter for reducing errors caused by misclassified (snow/cloud) pixels on the periphery of different land-cover classes. In total, 90–95% of cloud cover could be removed from the product, which improved it substantially.

## Accuracy Assessment

### Absolute accuracy

Absolute accuracy assessment was carried out as outlined above using station data from China. Station data were available for two years (2003 and 2004) from 168 stations and contained, apart from geographical information, snow depth and snow water equivalent. First, the data were converted to binary (snow or no snow) format consistent with the

Figure 10: Assessment of different filter constructs for optimising spatial filtering

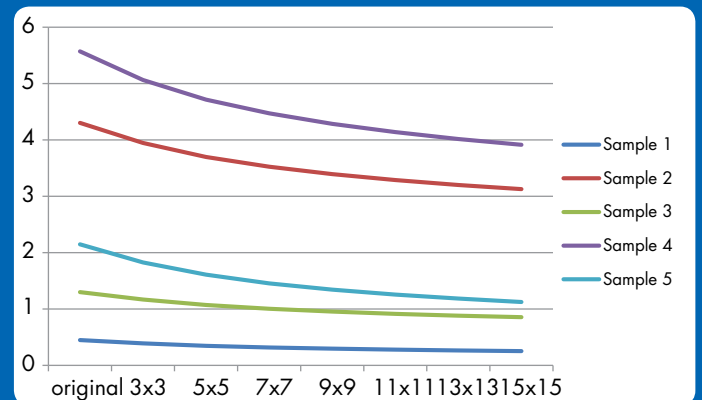


Figure 11: Profile of cloud cover area (%) after applying different filters

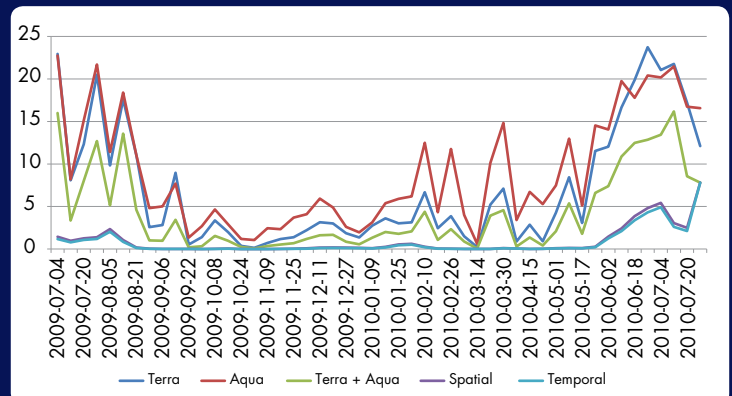
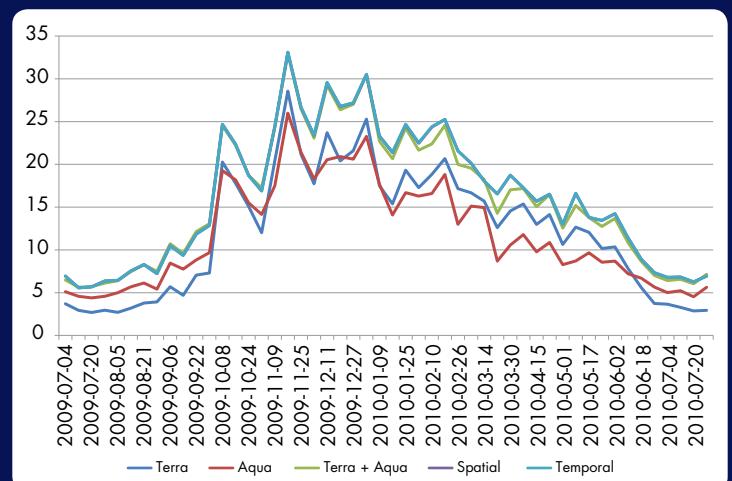


Figure 12: Profile of SCA (%) after applying different filters



MODIS snow product. Due to missing data, reference points were limited.

Accuracy assessment was carried out in Erdas Imagine 9.2 using five sets of reference data spanning five different months (Table 5). The best result obtained was for January 2004, with an overall accuracy of 97%, and the worst for November 2003, with an overall accuracy of 46%. According to Ault et al. (2006), the lower accuracy estimation is related to the presence of thin (<10 mm depth) traces of snow.

### Relative accuracy assessment

The relative accuracy assessment was carried out as described above. The overall accuracy of the enhanced MODIS 8-day composite in comparison to the 5-day composite was 93%.

**Table 5: Absolute accuracy of the 8-day enhanced MODIS product**

| Product date | No. of points | Overall accuracy | Kappa statistics |
|--------------|---------------|------------------|------------------|
| 17.11.2003   | 28            | 46.15%           | 0.1034           |
| 01.12.2003   | 41            | 97.30%           | 0.9165           |
| 15.01.2004   | 95            | 54.95%           | 0.2196           |
| 15.02.2004   | 71            | 73.53%           | 0.4383           |
| 16.03.2004   | 68            | 92.19%           | 0.4161           |

# Snow Cover Status

## Hindu Kush-Himalayan Region

The HKH region (Figure 1) comprises the mountainous areas of eight countries and has a total area of 4.19 million sq.km. The average SCA of the HKH region over the nine years from 2002 to 2010 was 0.76 million sq.km, or 18.2% of the total land area. The maximum and minimum SCA based on the 8-day SCA for 2002 to 2010 were 1.79 million and 0.15 million sq.km, 42.9 and 3.6% of the total land area, respectively. Monthly mean snow cover estimates showed maximum snow cover in February and least snow cover in July (Figure 13). February and July also had the maximum and minimum mean monthly variations respectively (Figure 14). The overall persistency over the nine years is shown in Figure 15.

## Variation in Snow Cover Area

### Interannual variation

Interannual variation in SCA was analysed for the years 2002 to 2010 using average annual values (Figure 16). Linear regression analysis showed a negative trend in interannual variation, but the results were not statistically significant. The maximum SCA was in 2005 and the minimum in 2010. A similar study showed a 16% decrease in SCA in the Himalayas from 1990 to 2001 (Menon et al. 2010).

Figure 13: Mean monthly SCA in the HKH

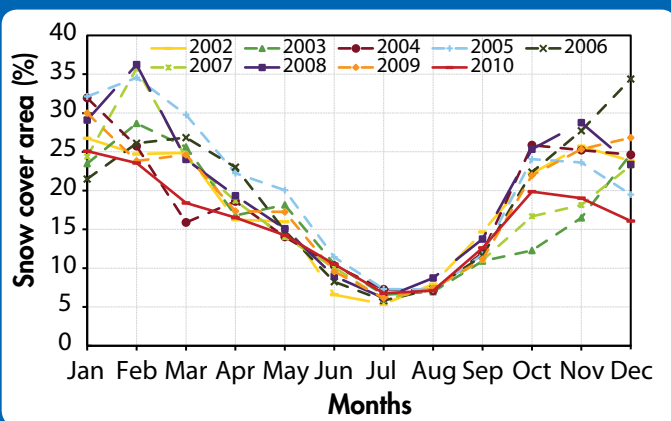


Figure 14: Monthly mean variation in SCA, 2002–2010

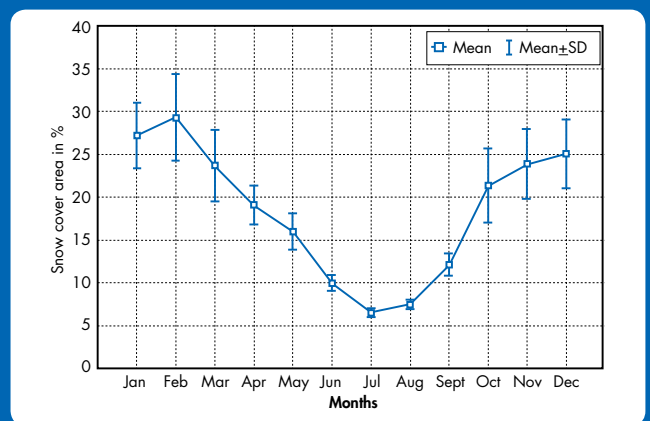


Figure 15: Snow cover persistency in the HKH region, 2002–2010

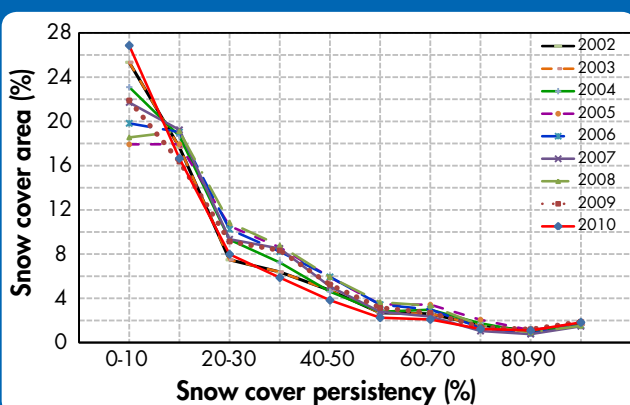


Figure 16: Average variation in SCA in the HKH region, 2002–2010

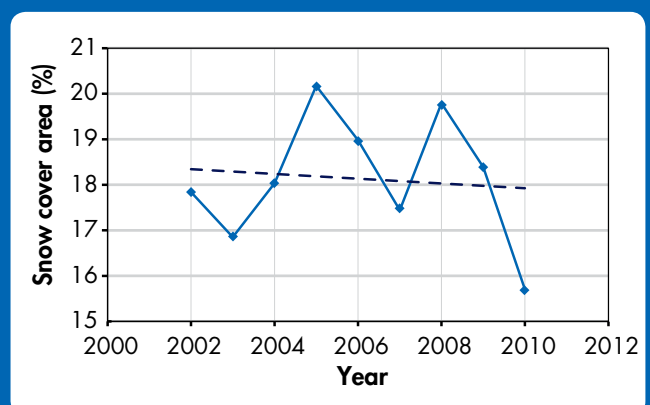
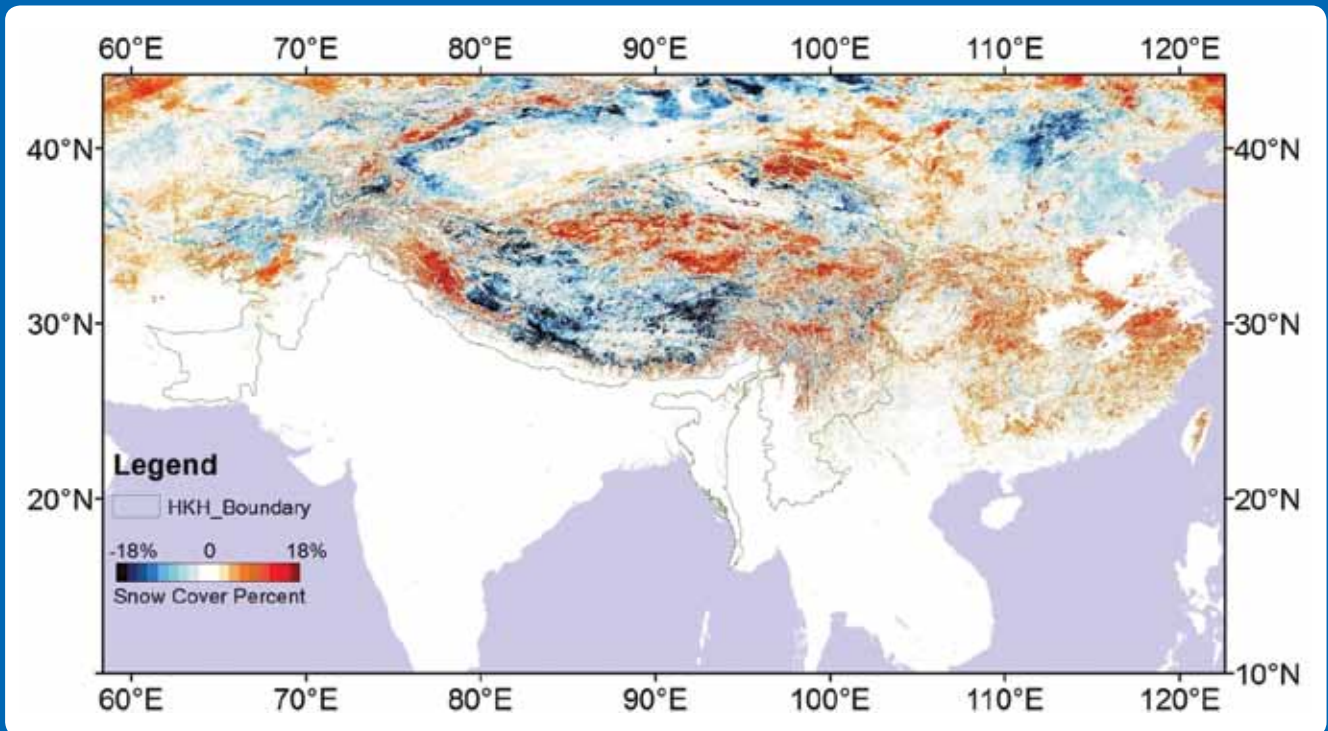


Figure 17: Changes in SCA in the HKH region and beyond, 2002–2010



A map was generated showing the percentage change in SCA from 2002 to 2010 in different parts of the HKH using a linear regression equation (Figure 17). The picture varied across the region. The central HKH showed a reduction of 14 to 18% in SCA, whereas some areas in the western and eastern HKH region showed increases of 10 to 12%.

Elevation plays an important role in snow accumulation and ablation. Interannual variation of snow cover was analysed for 16 different elevation zones of 500 m each (Figure 18). Linear regression analysis of annual mean SCA showed a positive trend at elevations below 3,500 m and a declining trend between 3,500 and 7,000 m, beyond which it again increased. The trends however were not statistically significant.

Figure 19 shows the mean SCA variation as a function of slope within different elevation zones. It was more than 50% for the altitude class from 2,000 to 6,000 m and slope class greater than 30%. For altitudes higher than 6,000 m, SCA was 90% in all slope classes.

Most of the air moisture is conveyed from the tropical region in the south, which leads to intensive snowfall caused by terrain and/or orographic lifting on the southward slope along the southern edge of the HKH. According to Pu and Xu (2009), the northward slope receives less snowfall during autumn and winter. Although the southward slope receives more solar radiation, the snow-albedo effect can maintain a relatively large snow cover on that aspect.

The distribution of SCA was evaluated based on terrain aspect for the winter months December to March (Figure 20). There was no clear trend in SCA for altitude classes greater than 6,000 m. Depletion of snow was observed from December to March for elevations between 2,000 and 4,000 m, and accumulation for elevations from 4,000 to 6,000 m that were more prominent on the east-west aspect.

Persistency of snow was evaluated for each month to see what elevation of land area was under snow cover during the period 2002–2010 (Figure 21). For altitudes above 3,500 m, two peaks were observed for 90% snow persistency in the winter from December to March. This pattern was not observed during other seasons or months.

Figure 18: Interannual variation in SCA for each 500 m of elevation

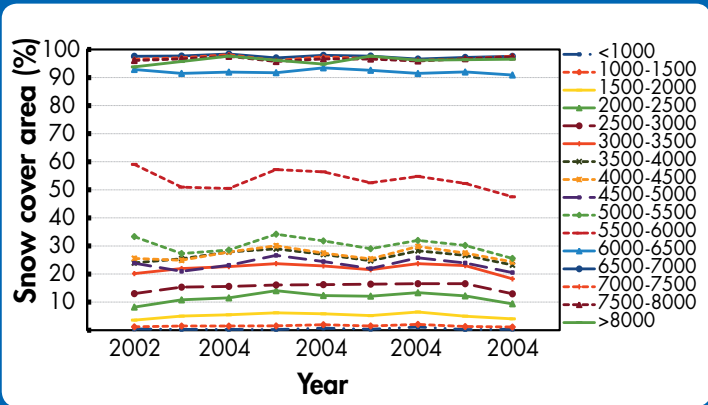
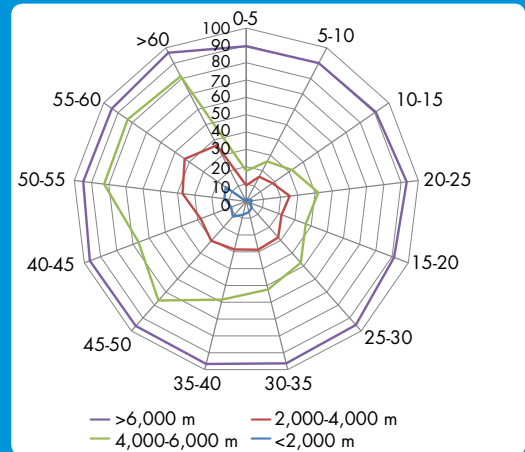
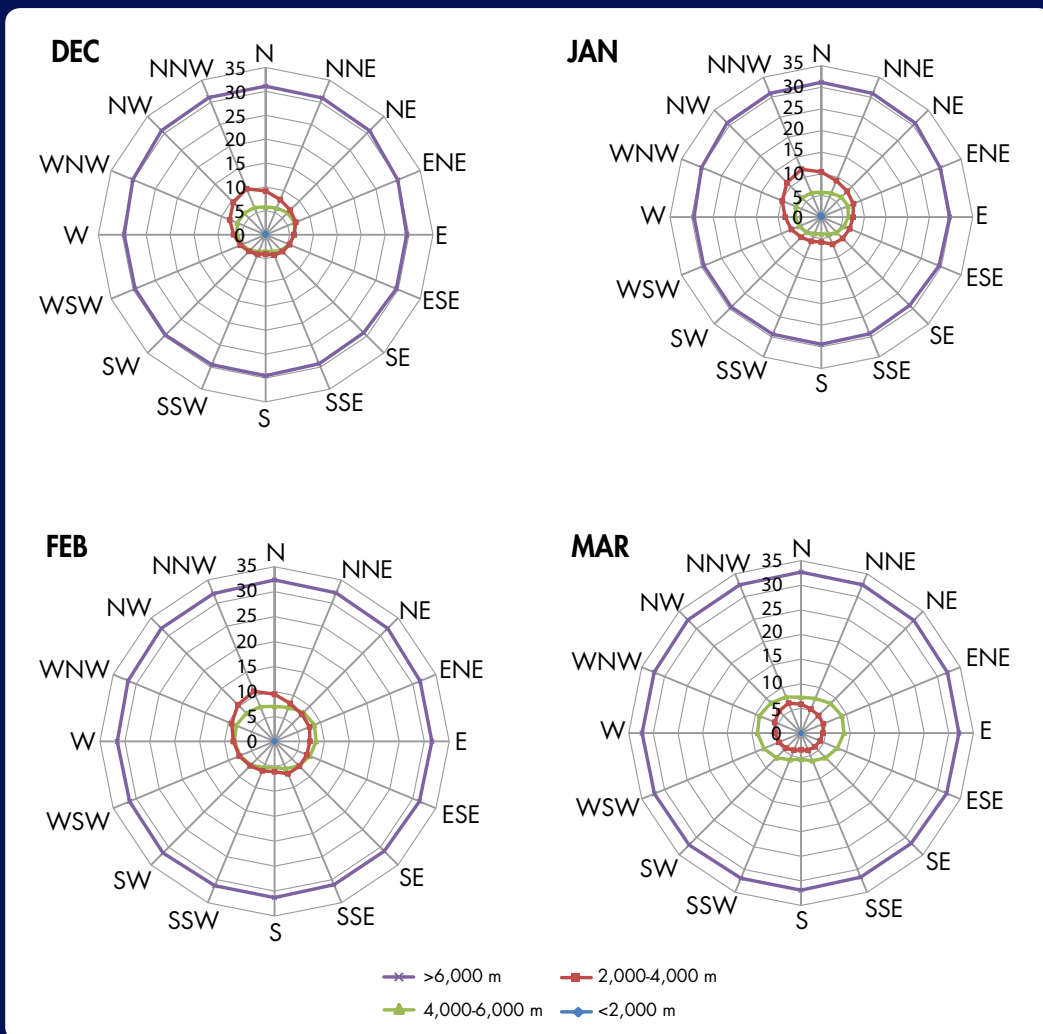


Figure 19: Distribution of snow cover in relation to elevation and slope



The radius in the polar coordinate shows the SCA (%) and the angles (degree) indicate slope classes. The four curves are the mean SCA for the elevation ranges below 2,000 m, at 2,000–4,000 and 4,000–6,000 m, and above 6,000 m.

Figure 20: Monthly variation (December to March) in SCA based on elevation and aspect classes



The radius in the polar coordinate shows the SCA (%) and the text indicates aspect classes. The four curves are the mean SCA for the elevation ranges below 2,000 m, at 2,000–4,000 and 4,000–6,000 m, and above 6,000 m.

Figure 21: Monthly snow cover persistence for the HKH region using enhanced MODIS snow-cover products, 2002–2010

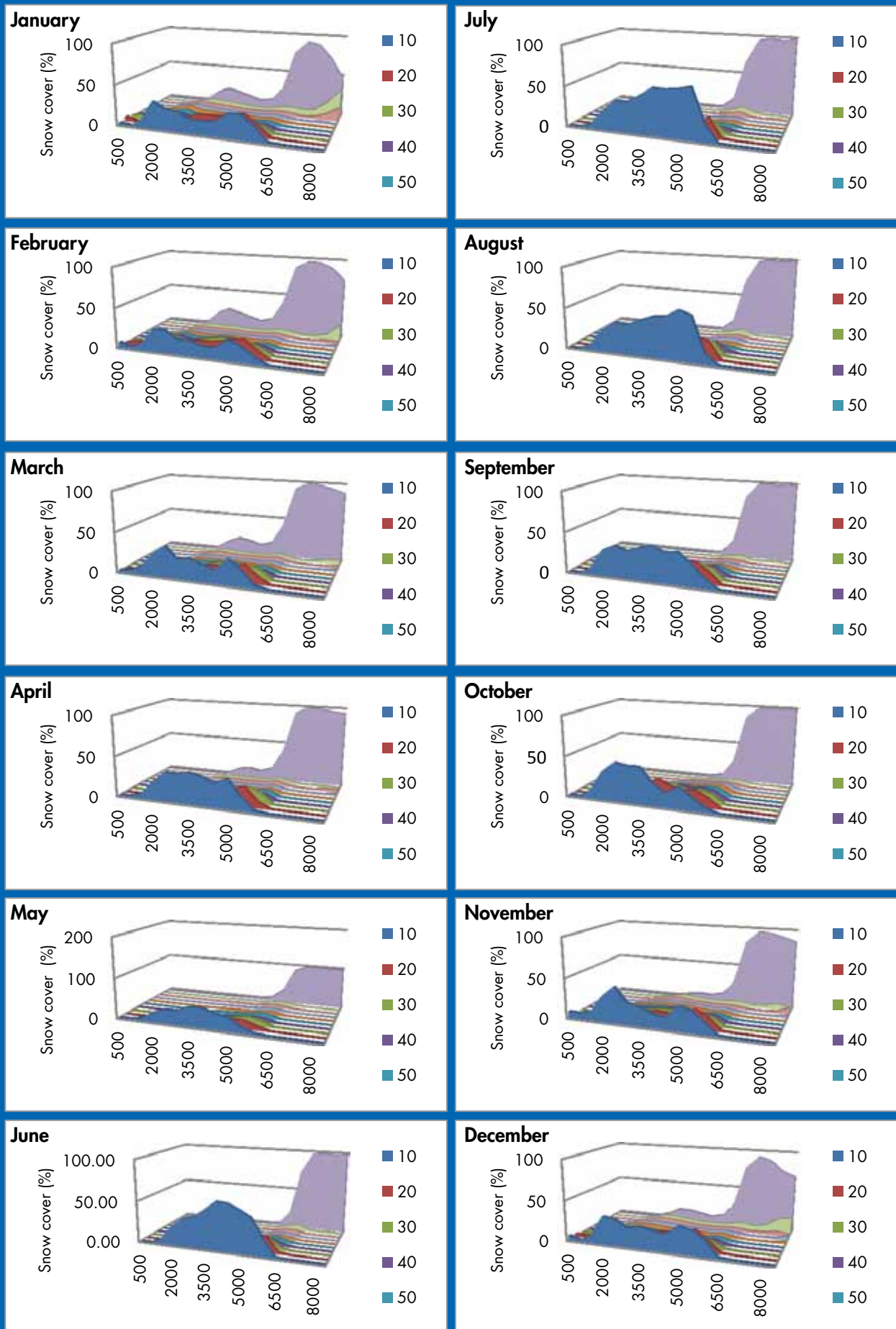
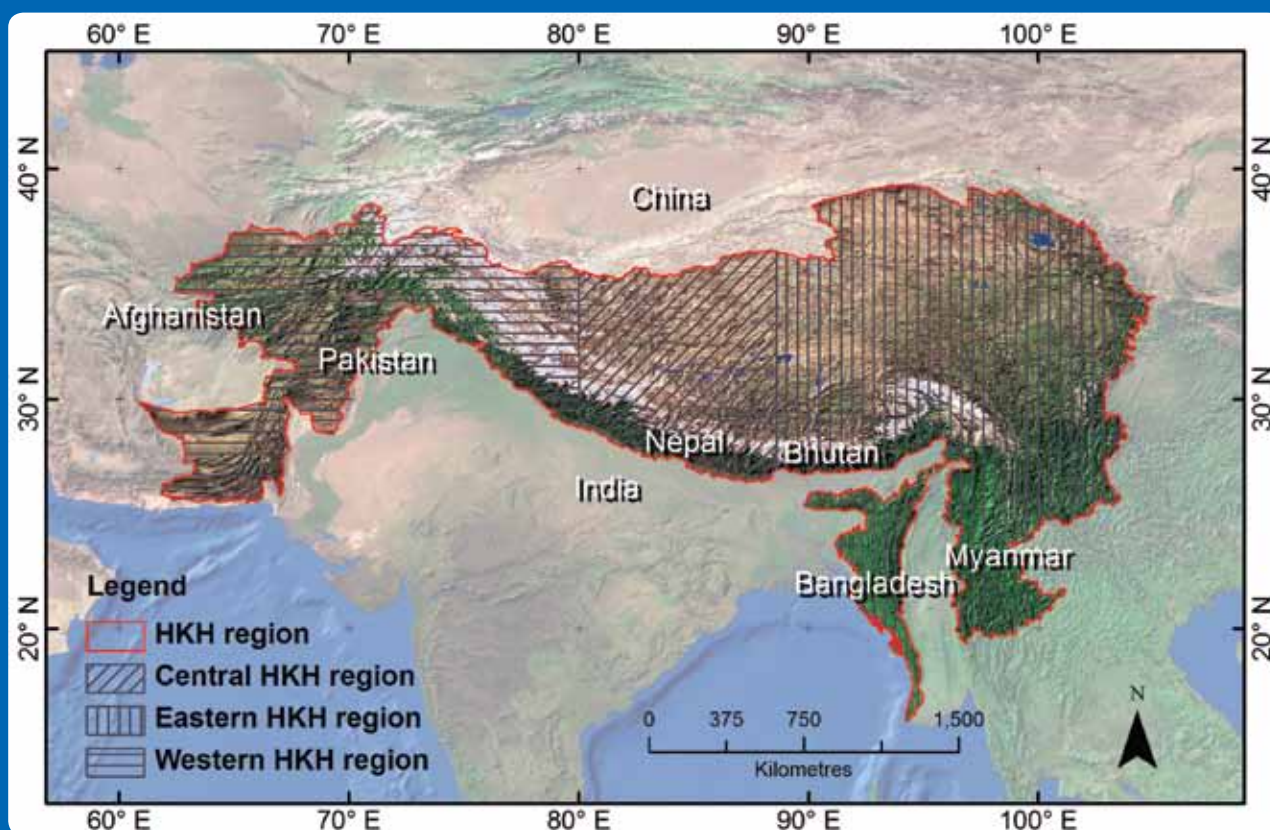


Figure 22: Snow cover analysis disaggregated into western, central, and eastern parts of the HKH region



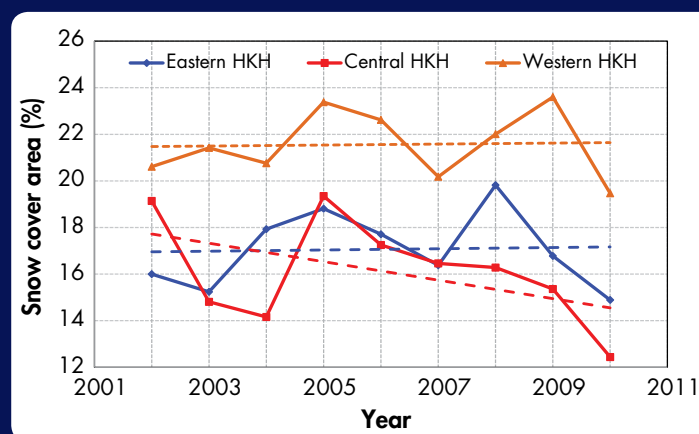
As a result of the climatic heterogeneity and diverse topography across the HKH region, generalised snow cover statistics across the whole region are unlikely to reflect clearly the trends and distribution patterns on the ground. Thus the SCA was further analysed for different parts of the region: the western HKH, central HKH, and eastern HKH (Figure 22). Delineation of these different regions was based on references such as the Atlas of the Himalaya (Zurick et al. 2005). The results are shown in Figure 23.

The SCA trend across the HKH region was not statistically significant. However, the values indicated a possible tendency towards a declining trend in the central HKH region (and the HKH overall) and an increasing trend in the western and eastern regions (Table 6).

#### Intra-annual variation

The mean annual SCA for the nine years from 2002 to 2010 showed a variation ranging from 0.66 million sq.km in 2010 to 0.85 million sq.km in 2005. The difference between maximum and minimum 8-day SCA was highest in 2006 and lowest in 2010 (Table 7). The mean monthly SCA values were in agreement

Figure 23: Interannual snow cover trends for the western, central, and eastern parts of the HKH region



The broken line indicates the trend based on linear regression equation.

Table 6: Annual snow cover trends in the western, central, and eastern HKH regions (%)

| HKH region   | Western HKH | Central HKH  | Eastern HKH |
|--------------|-------------|--------------|-------------|
| -0.05 ± 1.32 | 0.02 ± 1.36 | -0.40 ± 1.86 | 0.03 ± 1.55 |

**Table 7: Summary of annual SCA for the period 2002–2010 (sq.km)**

| Year    | 2002      | 2003      | 2004      | 2005      | 2006      | 2007      | 2008      | 2009      | 2010      |
|---------|-----------|-----------|-----------|-----------|-----------|-----------|-----------|-----------|-----------|
| Mean    | 747,766   | 706,342   | 755,830   | 845,493   | 795,502   | 731,155   | 829,501   | 770,782   | 658,239   |
| Minimum | 152,962   | 211,362   | 255,894   | 256,011   | 205,209   | 219,209   | 241,862   | 233,897   | 225,213   |
| Maximum | 1,478,336 | 1,459,252 | 1,575,576 | 1,564,823 | 1,799,413 | 1,677,666 | 1,775,934 | 1,653,997 | 1,281,207 |

**Table 8: Scheme adopted for analysing seasonal trends**

| Season | Month                |
|--------|----------------------|
| Winter | December to March    |
| Spring | April to June        |
| Summer | July to September    |
| Autumn | October and November |

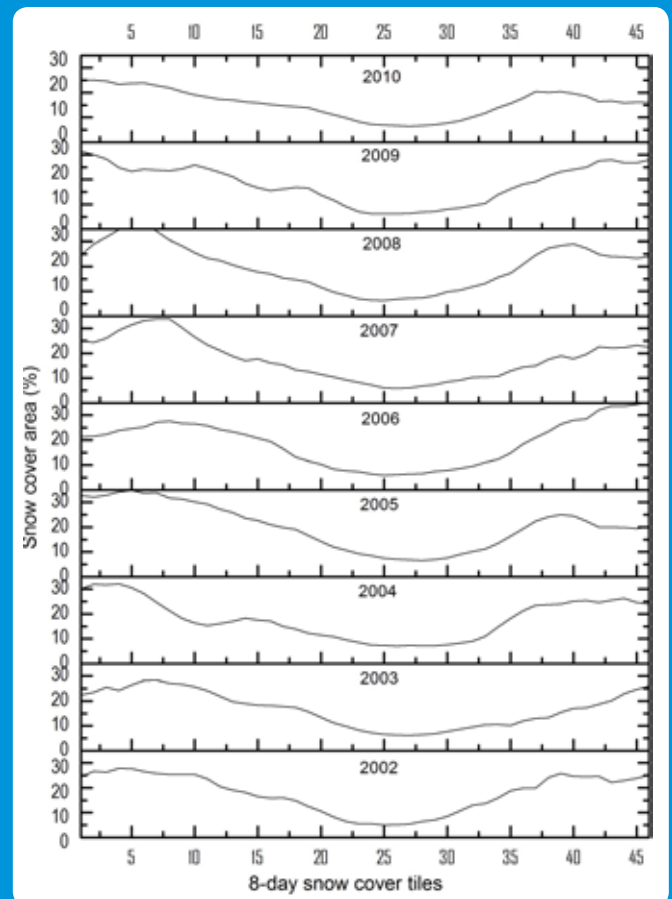
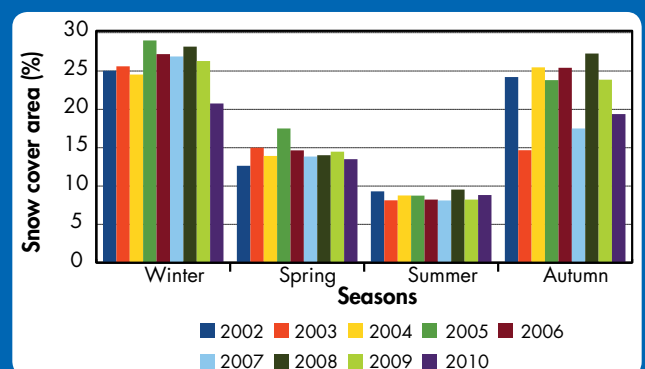
with the annual trend in snowfall. The intra-annual trends for 2002 to 2010 (Figure 24) do not indicate any significant deviation; there are only subtle differences. July had the lowest SCA, whereas in most years February had the highest SCA. However, nine years is not sufficient to identify any impacts of climate change on snowfall patterns.

### Seasonal variation

Seasons play an important role in snow dynamics. Equally, the great contrast in topographical relief results in numerous small climatic differences over short horizontal distances. The seasonal dynamics in snowfall pattern were analysed using a scheme for seasons adapted from previous studies (Immerzeel et al. 2009, Jain et al. 2009) (Table 8).

The seasonal SCA in different years is shown in Figures 24 and 25. The maximum snow cover was in winter followed by autumn, spring, and summer, consistent with the observations of Immerzeel et al. (2009). On average, SCA in winter was 27%, and in summer 7%. The interannual variation of seasonal mean SCA was least in summer and most in autumn (Figure 26).

The SCA trends obtained for the individual seasons across different parts of the region were not statistically significant (Table 9). However, there was an indication that SCA was decreasing over the eastern, central, and whole region in spring, consistent with the findings of previous studies in the Himalayas (Kripalani et al. 2003) and globally (Brown 1997), but increasing in the western HKH; and that SCA was decreasing in all areas in winter, consistent with the observations by Immerzeel et al. (2009) in the upper Indus basin.

**Figure 24: Intra-annual variations in snow cover area in the HKH, 2002–2010****Figure 25: Seasonal SCA, 2002–2010**

**Table 9: Seasonal snow cover trends in the HKH region (%)**

| Season | HKH region   | Western HKH  | Central HKH  | Eastern HKH  |
|--------|--------------|--------------|--------------|--------------|
| Spring | -0.03 ± 1.28 | +0.11 ± 1.83 | -0.23 ± 2.46 | -0.03 ± 1.06 |
| Summer | -0.01 ± 0.49 | +0.16 ± 0.65 | -0.20 ± 1.40 | -0.04 ± 0.52 |
| Autumn | +0.09 ± 3.97 | -0.26 ± 2.81 | +0.02 ± 5.74 | +0.29 ± 5.32 |
| Winter | -0.16 ± 2.23 | -0.02 ± 2.80 | -0.84 ± 2.63 | -0.01 ± 2.47 |

The land area under different percentages of snow cover during the period 2002 to 2010 was assessed for the entire HKH region in all four seasons. Less than 5% of the total land area had snow cover for more than 50% of the total period, and only 2% was always covered with snow (100% of the period). Similar snow persistency analysis for different seasons (Figure 27) varied across the seasons. Persistency was very low for summer months in general but higher for lower (10–20%) values. The autumn season had better snow persistency in general. Higher persistency was recorded during the winter months.

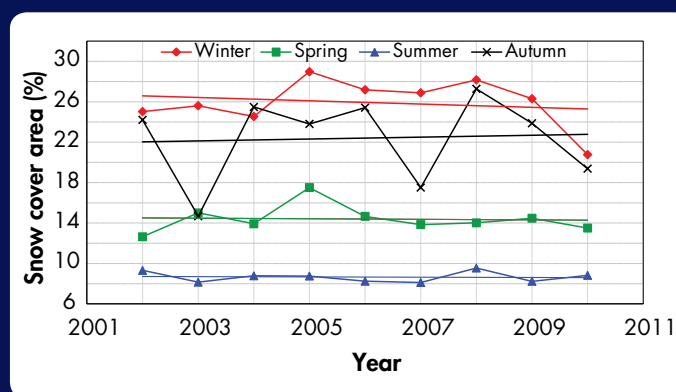
Table 10 shows the seasonal SCA trends in different elevation classes. None of the trends were statistically significant, and there was no indication of any pattern in SCA across the altitudinal belts.

Figure 28 shows the monthly variations in SCA for different elevation and slope classes in winter. Strong seasonal variations in SCA were found over the whole of the region. SCA for altitude classes from 2,000 to 4,000 m increased in January and February for slope classes above 40°; SCA for altitude classes from 4,000 to 6,000 m increased in February and March for slope classes above 50°. No seasonal variation or slope changes were observed for altitude classes above 6,000 m. The results indicate the extreme spatial variability in monthly snow cover resulting from the complex terrain.

### The Ten Major River Basins

Few studies have looked into snow cover trends and patterns on a regional scale in the HKH, and none so far have considered all ten of the major river basins. One of the most recent studies (Immerzeel et al. 2009) carried out an analysis of SCA using MODIS snow products for five of the ten major basins: the Brahmaputra, Indus, Ganges, Yangtze, and Yellow. Large spatial variations were identified in snow cover due to the vast differences in climate and altitude.

**Figure 26: Seasonal variation in SCA in the HKH region, 2002–2010**



**Figure 27: SCA for classes of snow occurrence in different seasons (%)**

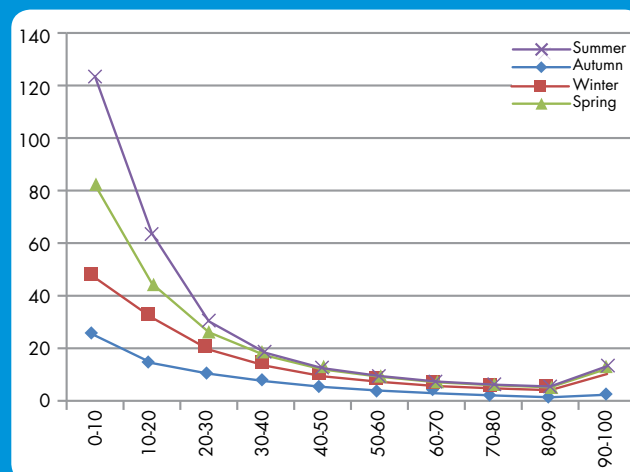
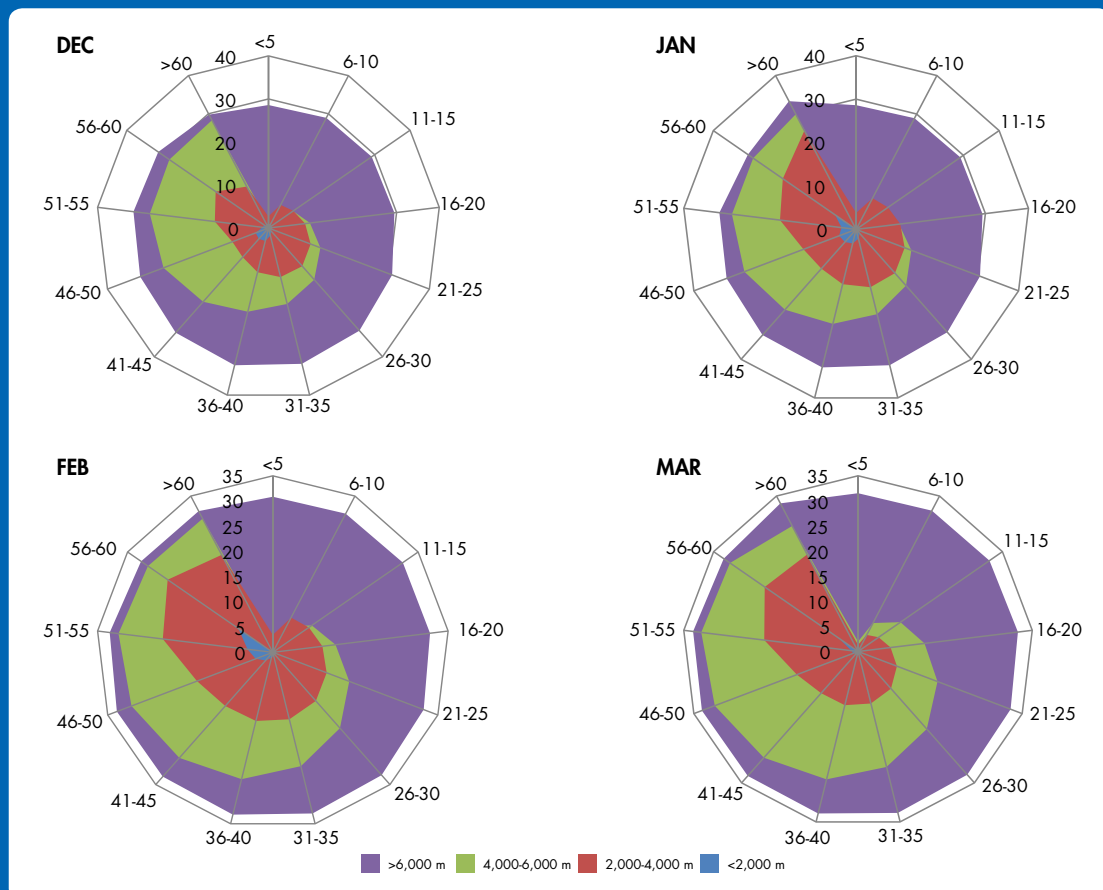


**Table 10: Snow cover trends in the HKH region in terms of season and elevation zone**

| Elevation Zone (m) | Winter (%)   | Spring (%)     | Summer (%)     | Autumn (%)    | Annual (%)   |
|--------------------|--------------|----------------|----------------|---------------|--------------|
| <1,000             | 0.06 ± 0.83  | 0.002 ± 0.01   | 0.00 ± 0.00    | 0.001 ± 0.08  | 0.02 ± 0.29  |
| 1,000-1,500        | 0.012 ± 0.81 | 0.013 ± 0.07   | 0.001 ± 0.07   | -0.011 ± 0.19 | 0.006 ± 0.30 |
| 1,500-2,000        | 0.12 ± 2.26  | 0.05 ± 0.27    | 0.0001 ± 0.25  | -0.036 ± 0.75 | 0.05 ± 0.88  |
| 2,000-2,500        | 0.49 ± 4.37  | 0.07 ± 0.56    | -0.005 ± 0.42  | -0.06 ± 1.47  | 0.18 ± 1.68  |
| 2,500-3,000        | 0.29 ± 2.89  | 0.15 ± 0.86    | -0.02 ± 0.33   | -0.24 ± 2.05  | 0.09 ± 1.34  |
| 3,000-3,500        | -0.07 ± 3.07 | 0.17 ± 1.90    | -0.006 ± 0.31  | -0.59 ± 3.42  | -0.07 ± 1.67 |
| 3,500-4,000        | -0.13 ± 3.35 | 0.13 ± 2.32    | 0.07 ± 0.52    | -0.35 ± 5.04  | -0.05 ± 1.89 |
| 4,000-4,500        | -0.20 ± 3.39 | 0.04 ± 2.00    | 0.16 ± 0.75    | 0.32 ± 6.52   | 0.03 ± 1.97  |
| 4,500-5,000        | -0.50 ± 2.78 | -0.02 ± 1.71   | 0.04 ± 0.78    | 0.69 ± 7.43   | -0.06 ± 1.94 |
| 5,000-5,500        | -0.61 ± 3.02 | -0.42 ± 3.35   | -0.29 ± 2.23   | 0.27 ± 9.23   | -0.35 ± 2.54 |
| 5,500-6,000        | -0.88 ± 3.22 | -0.59 ± 4.32   | -0.22 ± 3.37   | -0.89 ± 9.55  | -0.64 ± 3.05 |
| 6,000-6,500        | -0.29 ± 1.90 | 0.01 ± 1.09    | 0.01 ± 1.27    | -0.09 ± 1.81  | -0.11 ± 0.07 |
| 6,500-7,000        | -0.20 ± 1.35 | -0.0003 ± 0.10 | -0.0006 ± 0.23 | -0.02 ± 0.45  | -0.07 ± 0.45 |
| 7,000-7,500        | 0.004 ± 1.90 | 0.003 ± 0.10   | -0.001 ± 0.16  | -0.005 ± 0.75 | 0.001 ± 0.65 |
| 7,500-8,000        | 0.17 ± 1.59  | 0.03 ± 0.21    | -0.04 ± 0.13   | -0.06 ± 0.96  | 0.05 ± 0.57  |
| > 8,000            | 0.47 ± 2.97  | 0.00 ± 0.56    | -0.03 ± 0.32   | 0.23 ± 1.08   | 0.19 ± 1.06  |

**Figure 28: Snow cover area in terms of elevation and slope classes in winter (December–March)**



The radius in the polar coordinate demonstrates the SCA (%) and the angles (degree) indicate slope classes. The four curves are the mean SCA for the elevation ranges below 2,000 m, at 2,000–4,000 and 4,000–6,000 m, and above 6,000 m

The snow cover results calculated here for each of the ten major river basins of the HKH for the period from 2002 to 2010 are summarised in Table 11 – overall and seasonal trends in SCA; Table 12 – correlation between elevation and SCA; Figure 29 – basin area and snow extent; and Figure 30 – interannual variation in SCA. The area, average SCA, and mean elevation of the basins are summarised in Table 13. The geographical position of the basins is shown in Figure 5. The results for individual basins are discussed in the following sections.

### Amu Darya basin

The Amu Darya basin extends across parts of Afghanistan, Tajikistan, Turkmenistan, and Uzbekistan (King and Sturteagen 2010), and with an area of 645,895 sq.km is the seventh largest of the ten basins. The HKH mountain system forms the south and south-eastern limit of the basin and has extensive glacier and snow fields that recharge the river system network.

The Amu Darya basin had an average annual SCA of 9,918 sq.km, less than 2% of the basin area (Table 13). The minimum snowfall recorded was in 2007 and maximum in 2008 (Figure 30). The SCA trend for the period ( $-0.05 \pm 1.98\%$ ) was not statistically significant, nor was the seasonal trend (Table 11). Linear regression analysis showed a strong correlation between snow cover and altitude ( $R = 0.97$ ) (Table 12).

**Table 11: Average annual and seasonal trends in SCA in the ten major river basins, 2002–2010**

| Basin        | SCA Trend (%)    |                  |                  |                  |                  |
|--------------|------------------|------------------|------------------|------------------|------------------|
|              | 2002–2010        | Winter           | Summer           | Spring           | Autumn           |
| Amu Darya    | $-0.05 \pm 1.98$ | $-0.05 \pm 1.98$ | $0.10 \pm 0.98$  | $-0.02 \pm 1.73$ | $-0.39 \pm 3.11$ |
| Brahmaputra  | $-0.07 \pm 0.22$ | $-0.07 \pm 0.22$ | $-0.11 \pm 0.75$ | $-0.46 \pm 1.40$ | $-0.51 \pm 4.56$ |
| Ganges       | $0.02 \pm 0.20$  | $0.02 \pm 0.20$  | $0.01 \pm 0.12$  | $-0.04 \pm 0.26$ | $-0.04 \pm 0.64$ |
| Indus        | $-0.12 \pm 0.81$ | $-0.12 \pm 0.81$ | $0.15 \pm 0.48$  | $0.07 \pm 1.27$  | $-0.04 \pm 1.93$ |
| Irrawaddy    | $0.24 \pm 0.89$  | $0.24 \pm 0.89$  | $0.01 \pm 0.17$  | $0.01 \pm 0.20$  | $-0.04 \pm 0.30$ |
| Mekong       | $-0.02 \pm 1.82$ | $-0.02 \pm 1.82$ | $-0.01 \pm 0.12$ | $0.02 \pm 0.26$  | $0.10 \pm 0.90$  |
| Salween      | $-0.05 \pm 1.98$ | $-0.05 \pm 1.98$ | $-0.11 \pm 0.37$ | $-0.09 \pm 0.67$ | $0.08 \pm 3.94$  |
| Tarim        | $-0.31 \pm 1.05$ | $-0.31 \pm 1.05$ | $0.08 \pm 0.54$  | $-0.11 \pm 1.65$ | $0.50 \pm 2.20$  |
| Yangtze      | $-0.07 \pm 0.22$ | $-0.07 \pm 0.22$ | $0.01 \pm 0.30$  | $0.18 \pm 0.76$  | $0.46 \pm 1.87$  |
| Yellow River | $0.02 \pm 0.79$  | $0.02 \pm 0.79$  | $0.01 \pm 0.35$  | $0.03 \pm 0.69$  | $0.57 \pm 5.08$  |

**Table 12: Coefficient of correlation (*R*) between elevation and snow cover area for the ten major river basins**

| Basin       | <i>R</i> <sup>2</sup> | <i>R</i> |
|-------------|-----------------------|----------|
| Amu Darya   | 0.95                  | 0.97     |
| Brahmaputra | 0.83                  | 0.91     |
| Ganges      | 0.91                  | 0.95     |
| Indus       | 0.93                  | 0.96     |
| Irrawaddy   | 0.97                  | 0.99     |
| Mekong      | 0.73                  | 0.86     |
| Salween     | 0.78                  | 0.88     |
| Tarim       | 0.82                  | 0.90     |
| Yangtze     | 0.76                  | 0.87     |
| Yellow      | 0.77                  | 0.87     |

**Figure 29: Basin area and snow extent in each of the ten major river basins**

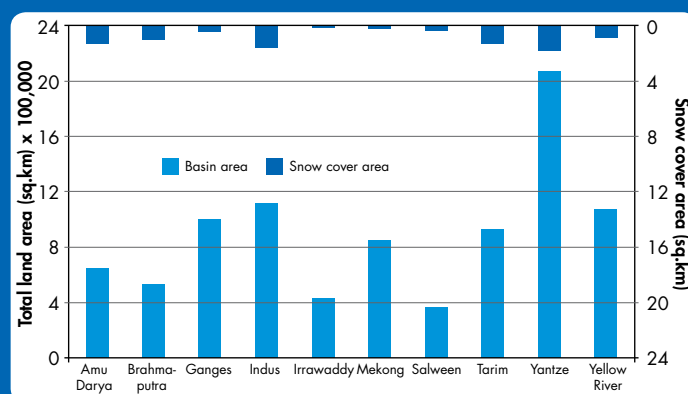
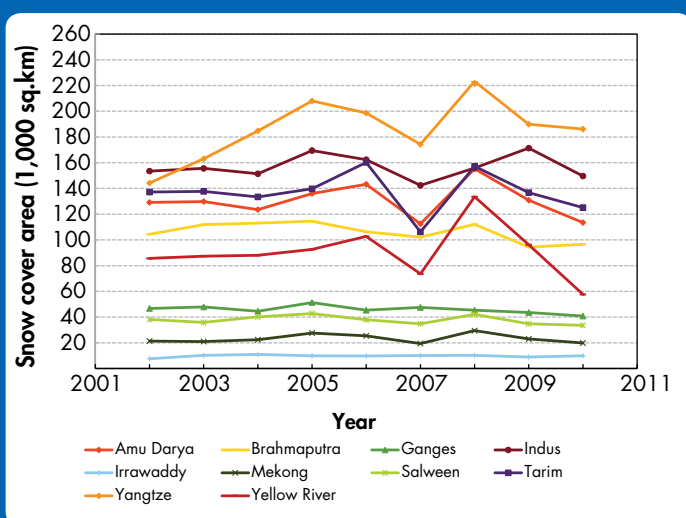


**Figure 30: Interannual variation in snow cover area for the ten major river basins**



### Brahmaputra basin

Originating in the High Himalayas, the Brahmaputra River flows 1,800 miles through Bangladesh, India, and the Tibet Autonomous Region in China. With a total area of 528,082 sq.km, the Brahmaputra basin is the eighth largest of the ten basins. Snow is important for maintaining the hydrological regime of the river. Using the Normalized Melt Index (NMI), defined as the volumetric discharge from snow and glaciers upstream divided by the downstream natural discharge, Immerzeel et al. (2010) showed that the contribution of snow compared to that of glaciers was significant in this basin.

The average SCA for the period was 107,121 sq.km, or 20.4% of the total basin area, the fourth largest basin in terms of average SCA, and largest in terms of percentage of SCA. The highest SCA was recorded in 2005 and the lowest in 2009 (Figure 30). The seasonal SCA trend, although not statistically

significant, indicated a tendency towards depletion in all four seasons. Snow distribution had a strong correlation with elevation ( $R = 0.91$ ).

### Ganges basin

The Ganges flows through China, Nepal, India, and Bangladesh. The river basin has an area of 1,001,087 sq.km, the fourth largest of the ten. The Himalayas limit the basin to the north forming the Ganges-Brahmaputra divide.

The average SCA in the basin was 47,742 sq.km, approximately 5% of the total area. The trends in SCA were not statistically significant, but indicated a positive annual trend for the decade ( $0.02 \pm 0.20\%$ ), with declining trends in winter and autumn (Table 11). There was a strong correlation between SCA and elevation ( $R = 0.95$ ).

**Table 13: Total area and average annual SCA of the ten river basins, 2002–2010**

| Basin        | Total land area (sq.km) | Average snow cover area |      | Mean elevation (masl) |
|--------------|-------------------------|-------------------------|------|-----------------------|
|              |                         | (sq.km)                 | (%)  |                       |
| Amu Darya    | 645,895                 | 9,918                   | 1.6  | 1,382                 |
| Brahmaputra  | 528,082                 | 107,121                 | 20.4 | 3,191                 |
| Ganges       | 1,001,087               | 47,742                  | 4.8  | 894                   |
| Indus        | 1,116,347               | 167,992                 | 16.7 | 1,587                 |
| Irrawaddy    | 426,393                 | 9,511                   | 2.4  | 716                   |
| Mekong       | 841,337                 | 23,534                  | 3.0  | 990                   |
| Salween      | 363,898                 | 38,571                  | 10.7 | 2,012                 |
| Tarim        | 929,254                 | 167,061                 | 15.9 | 2,223                 |
| Yangtze      | 2,066,050               | 193,304                 | 9.4  | 1,611                 |
| Yellow River | 1,073,443               | 95,193                  | 9.4  | 1,816                 |

## Indus basin

The Indus basin extends across parts of Afghanistan, China, India, and Pakistan, and with an area of 1,116,347 sq.km is the second largest river basin in Asia after the Yangtze basin. The rivers in the Indus basin are fed by snow and glacial melt and monsoon rain; the major component of the annual flow is derived from snowmelt, originating in the HKH region.

The average SCA was 167,992 sq.km, 16.7% of the total area. Although trends weren't significant, they indicated a slightly positive trend overall ( $0.02 \pm 0.79\%$ ), with a negative trend during winter and autumn and a positive trend in summer and spring (Table 11). There was a strong correlation between SCA and elevation ( $R = 0.96$ ).

## Irrawaddy basin

The Irrawaddy is Myanmar's biggest river. The river basin is ninth among the major river basins with an area of 426,393 sq.km (Table 13). The average decadal SCA was lowest of all the basins with a coverage of just 9,511 sq.km or 2.40% of the basin area. Although trends weren't significant, they indicated a slightly positive trend overall over the period 2002 to 2010 ( $0.02 \pm 0.20\%$ ), with a negative trend during autumn and a positive trend in winter, spring, and summer (Table 11). There was a strong correlation (coefficient 0.99) between SCA and elevation.

## Mekong basin

The Mekong originates in the snow-capped Tanggula Shan Mountains of the Tibet Autonomous Region in China and flows through the six countries of China, Myanmar, Laos, Thailand, Cambodia, and Vietnam. Snow is a major source of runoff, particularly during the dry season. Snowmelt helps to maintain the dry season flows. The basin has a total area of 841,337 sq.km, sixth largest of the ten river basins.

The average SCA in the river basin was 23,534 sq.km, 3% of the total area and eighth in terms of average SCA percentage (Table 13). While not significant, the SCA trend for the period 2002 to 2010 ( $0.01 \pm 0.39\%$ ) indicated an increasing trend overall, with a decreasing trend for summer and winter and increasing trend in spring and autumn (Table 11). The correlation coefficient between SCA and elevation was good (0.86).

## Salween basin

The Salween River originates from the Tanggula Mountains in the Tibetan plateau, flows southwards through Yunnan Province in China and the Shan and Kayah states of eastern Myanmar, along the Thai-Myanmar border passing through the Kayan and Mon states of Myanmar, and finally empties into the Gulf of Martaban in the Andaman Sea. Snow is present in the upper catchment.

The basin has a total area of 360,297 sq.km, the smallest among the ten basins, and an average SCA of 38,571 sq.km or 10.7% of the total area. There was a decreasing trend in SCA ( $-0.12 \pm 0.81\%$ ), although not statistically significant, with a decreasing trend in winter, summer, and spring, and a positive trend in autumn. The correlation coefficient between SCA and elevation was good (0.88).

## Tarim basin

The Tarim Basin is a large endorheic basin (with no outflow to a river or ocean) covering an area of more than 929,254 sq.km, fifth largest of the ten basins. It is bounded by the Tian Shan mountain range to the north, and the Kunlun mountains with the Tibetan Plateau on their northern edge, to the south. The tributaries in the Tarim basin have their source in the snow-clad mountain ranges.

The Tarim basin had an average SCA of 167,061 sq.km, 15.9% of the total land area (Table 13). Although not statistically significant, the SCA trend indicated a negative effect overall ( $-0.07 \pm 1.62\%$ ), with a negative trend in

winter and spring and a positive trend in summer and autumn (Table 11). The correlation coefficient between snow cover area and elevation was good (0.90).

### Yangtze basin

The Yangtze River is 6,300 km long, the eleventh longest river in the world. With an area of 2,066,050sq.km, the river basin is by far the largest of the ten originating in the HKH. The Yangtze river is fed by snow from the Kunlun mountains, the Tibetan Plateau, and surrounding mountain areas, and flows into the East-China Sea.

The Yangtze River basin had the highest average SCA of all the basins at 193,304 sq.km, 9.41% of the total basin area. Although not statistically significant, the SCA trend indicated a positive value for all seasons as well as over the whole period, in contrast to the other nine basins (Table 11). The correlation coefficient between SCA and elevation was good (0.87).

### Yellow River basin

The Yellow River has its source in the Qinghai-Tibetan plateau of Qinghai province and flows across eight other provinces and autonomous regions before emptying into the Yellow Sea north of the Shandong Peninsula. With a length of over 5,400 km, the Yellow River is the second longest river in China and the tenth longest in the world (Giordano et al. 2004).

The Yellow River basin is third in the list in terms of both basin area (1,073,443 sq.km) and average SCA (95,193 sq.km or 9.40% of the total area). A (non-significant) decreasing trend was observed in SCA over the whole period and in the winter, with a positive trend in summer, spring and autumn (Table 11). The correlation coefficient between SCA and elevation was good (0.87).

# Discussion

## The Snow-Mapping Algorithm

Developing and validating a new algorithm and having it endorsed by the scientific community is a protracted and rigorous process. Thus the results described in this publication were developed using the global snow mapping algorithm to gain an overall approximation of the snow cover in the region and trends over the past decade while work on customising the algorithm continued in parallel.

The results show that the original algorithm using the global MODIS snow product overestimates SCA in the HKH region. In this algorithm, the effects of atmosphere, terrain, and viewing angle are not corrected. The algorithm also uses generalised threshold values, which may cause significant errors in estimation of snow cover in mountain areas, especially in extremely rugged terrain like that in the HKH region. Overestimation was observed, among others, in the appearance of snow pixels in the Terai where it is known that there is no snow. Some attempt was made to filter the results based, for example, on elevation. However, in the longer term it will be necessary to customise the snow algorithm to ensure that snow cover information is as credible and accurate as possible.

A customised algorithm has been prepared and is undergoing review. Once it is finalised, it will be used to prepare more accurate snow products for the region, and the degree of error in the present results will also be calculated.

## Spatial Visualisation and Dissemination System

The 8-day enhanced snow cover maps for the HKH region and the ten major downstream river basins provide vital information that will be useful in bridging the data gap on snow cover in the region. It is important to ensure that the data and products are easily accessible so that they can be used to support research on climate change and climate change adaptation, as well as for more immediate local purposes. An interactive web-based platform has been developed and is being tested for use as a single gateway to data and information. The application focuses on spatial visualisation and geo-statistical surface analysis of snow-cover mapping in the HKH region, including the ten major downstream river basins and 92 sub-basins. The system is being implemented in ArcGIS Server 10 from ESRI to serve both vector and raster GIS layers. It is expected to be implemented for open access in 2011.

## Applications

The high temporal and spatial resolution of the MODIS snow-cover product offers opportunities for use in a variety of applications, particularly for assessment of water resources. MODIS data on snow cover have been shown to improve the performance of snow models when validated against independent data on ground snow depth (Parajka and Blöschl 2008), and the daily snow cover maps have been used in the calibration of models (Konz et al. 2010).

## Hydrological Modelling: A case study

Snow plays a vital role in the energy and water budgets of drainage basins in the Himalayan region. Snow and glacier melt constitute 50 to 90% of the total river discharge in some major rivers systems during the dry season (Konz et al. 2010). Hydrological modelling in the Himalayan region is very difficult owing to the limited data available from the sparse observation networks and the enormous spatial variability of runoff formation factors such as snow processes. Satellite data such as MODIS snow cover can help compensate for the lack of field-based data.

The use of MODIS snow data for hydrological modelling and estimation of discharge was demonstrated in a pilot experiment for the Langtang Khola catchment in Nepal using a tracer-aided catchment-distributed (TAC-D) model and MODIS daily snow cover data for five hydrological years (January 2002 to May 2006). The test showed improved model efficiency using the snow cover maps relative to a previous application without the MODIS data.

# Conclusions and Recommendations

Climate science needs long-term data to predict future trends. Several researchers (Immerzeel et al. 2009; Jain et al. 2009; Kulkarni et al. 2010) have expressed the need for snow data over a longer term than currently available as a basis for credible research on climate change. The decade-long repository of snow data from MODIS is a first step in addressing this need. This needs to be maintained and expanded as more data become available. In addition, to give continuity to the mapping of snow using MODIS snow products, the data repository needs to be enriched with historical data on snow.

The global MODIS snow algorithm has some limitations for use in the HKH region which results in overestimation of snow cover. The improved algorithm now being developed, customised to the HKH context, will soon enable more accurate snow products to be developed for the HKH region.

The maps and trend analysis of SCA described here provide a first comprehensive assessment of snow cover across the Hindu Kush-Himalayan region. The global snow cover products still have scope for further improvement in terms of accuracy, but they provide a good first assessment of snow cover status and an indication of where efforts should be focused. Similarly, although the nine-year data set is not sufficient to generate statistically significant data on trends, the results do provide some indication of possible trends, and demonstrate the usefulness of the method and the potential for application as longer time series become available and the algorithm is improved.

Snow cover is one factor among a range of environmental data needed to understand the complex system of climate and other change. Several terrestrial and atmospheric data sets have been derived from MODIS. In future, it would be useful to expand the 'integrated tool for MODSPAT' to process other products in addition to snow.

Access to data is another important aspect which needs addressing. In this case, it will be important to develop appropriate ways to share the snow data. The planned cryosphere web portal should include dynamic spatial analysis tools such as fly clipping and extraction based on area of interest to facilitate area and user-specific analyses. Issuing of a regular snow bulletin for the region is also being considered.

Hydrological runoff models for estimation of water resources should be promoted and the use of snow-cover data should be encouraged. A pilot case study should be implemented in close consultation with partner institutes in different regional countries to create awareness about the usefulness of the data.

It is in the interest of the countries of the HKH region to ensure transfer of technology and knowledge to regional partners. Through this project ICIMOD has acquired the capacity to map and monitor snow cover. The countries of the region will be encouraged to take ownership of the process by using tools established in their own areas. Capacity building for partner institutes in the form of training and exchange visits may be useful.

In summary, the following recommendations are made to ensure that the work on snow cover estimation in the HKH region continues in the way needed to provide the critical results necessary for input into long-term models of climate change, as well as shorter-term mapping and modelling to predict future changes in water supply, among other topics, in the region.

- The present work in generating MODIS snow-cover products should be continued and put into operation as an automated system.
- Historical snow-cover data, such as AVHRR, should be accessed and processed for the HKH region to go back in time and generate snow cover data over a longer temporal framework.
- The new snow algorithm under review should be implemented and used to generate improved and reliable snow-cover products for the HKH region for assessment and use in environmental modelling.

- MODSPAT should be expanded and used for other MODIS products.
- A dynamic online system should be developed as an enterprise environment in the form of a single gateway to ensure wider dissemination of products.
- Information about snow cover should be compiled and disseminated in the form of a regular bulletin.
- Pilot case applications should be undertaken for hydrological modelling using snow data.
- Training should be provided for regional member organisations and exchange visits encouraged and supported.

# References

- Ackerman, SA; Strabala, KI; Menzel, WP; Frey, RA; Moeller, CC; Gumley, LE (1998) 'Discriminating clear sky from clouds with MODIS'. *Journal of Geophysical Research* 103(D24): 32141–32157
- Ault, T; Czajkovski, K; Benko, T; Coss, J; Struble, J; Spongberg, A; Templin, M; Gross, C (2006) 'Validation of the MODIS snow product and cloud mask using the student and NWS cooperative station observations in the Lower Great Lakes Region.' *Remote Sensing of Environment* 105: 341–353
- Brown, RD (1997) 'Historical variability in northern hemisphere spring snow-covered area.' *Annals of Glaciology* 25: 340–346
- Brown, RD (2000) 'Northern hemisphere snow cover variability and change, 1915–97.' *Journal of Climate* 13(13): 2339–2355
- Dahe, Q; Shiyin, L; Peiji, L (2006) 'Snow cover distribution, variability, and response to climate change in Western China.' *Journal of Climate* 19: 1820–1833
- Gafurov, A; Bardossy, A (2009) 'Cloud removal methodology from MODIS snow cover product'. *Hydrology and Earth System Sciences* 13(7): 1361–1373
- Giordano, M; Zhu, Z; Cai, X; Hong, S; Zhang, X; Xue, Y (2004) *Water management in the Yellow River basin: Background, current critical issues and future research needs*, Comprehensive Assessment Research Report 3. Colombo: Comprehensive Assessment Secretariat. [www.ivmi.org/assessment](http://www.ivmi.org/assessment)
- Hall, DK; Riggs, GA; Salomonson, W; DiGirolamo, NE; Bayr, KJ (2002) 'MODIS snow-cover products'. *Remote Sensing of Environment* 83(1–2): 181–194
- ICIMOD (2009) *Regional consultative workshop on remote sensing of the cryosphere – Assessment and monitoring of snow and ice in the Hindu Kush Himalayan (HKH) region*, Kathmandu, 31 March – 2 April 2009, workshop report. Kathmandu: ICIMOD
- Immerzeel, WW; Droogers, P; de Jong, SM; Bierkens, MFP (2009) 'Large-scale monitoring of snow cover and runoff simulation in Himalayan river basins using remote sensing.' *Remote Sensing of Environment* 113: 40–49
- Immerzeel, WW; van Beek LPH; Bierkens, MFPI (2010) 'Climate change will affect the Asian water towers.' *Science* 328: 1382–1385
- Ives, JD; Shrestha RB; Mool, PK (2010) *Formation of glacial lakes in the Hindu Kush-Himalayas and GLOF risk assessment*. Kathmandu: ICIMOD
- Jain, S; Goswami, A; Saraf, A (2009) 'Role of elevation and aspect in snow distribution in Western Himalaya.' *Water Resources Management* 23: 71–83
- Kaur, R; Saikumar, D; Kulkarni, AV; (2009) 'Variations in snow cover and snowline altitude in Baspa basin.' *Current Science* 96 (9): 1255–1258
- King, M; Sturtewagen, B (2010) *Making the most of Afghanistan's river basins: Opportunities of regional cooperation*. New York: EastWest Institute
- Konz, M; Finger, D; Buergi, C; Normand, S; Immerzeel, WW; Merz, J; Giriraj, A; Burlando, P (2010) 'Calibration of a distributed hydrological model for simulations of remote glacierised Himalayan catchments using MODIS snow cover data.' In *Global Change: Facing Risks and Threats to Water Resources* (Proc. of the Sixth World FRIEND Conference, Fez, Morocco, October 2010), IAHS Publication 340, pp 465–473. Wallingford, UK: International Association of Hydrological Sciences
- Kripalani, RH; Kulkarni, A; Sabade, SS (2003) 'Western Himalayan snow cover and Indian monsoon rainfall: A re-examination with INSAT and NCEP/NCAR data.' *Theoretical and Applied Climatology* 74: 1–18
- Krishna, AP (2005) 'Snow and glacier cover assessment in the high mountains of Sikkim Himalaya.' *Hydrological Processes* 19: 2375–2383
- Kulkarni, AV; Rathore, BP; Alex, S (2002) 'Is global warming changing snow ablation pattern and reducing glacial extent of Baspa basin in the Himalaya?' *ISPRS and SIS* 37(7): 1265–1269
- Kulkarni, AV; Singh, SK; Mathur, P; Mishra, VD (2006) 'Algorithm to monitor snow cover using AWiFS data of RESOURCESAT-1 for the Himalayan region.' *International Journal of Remote Sensing* 27(12): 2449–2457
- Kulkarni, AV; Rathore, BP; Singh, SK (2008) 'Monitoring of seasonal snow cover in the Western Himalaya.' In Venkataraman, G; Nagarajan, R (eds) *Proceedings of International workshop on snow, ice, glaciers and avalanches*, January 7–9, 2008, Mumbai, India, pp 85–92. New Delhi, India: Tata McGraw-Hill

- Kulkarni, AV; Rathore, BP; Singh, SK; Ajai (2010) 'Distribution of seasonal snow cover in central and western Himalaya.' *Annals of Glaciology* 51(54): 123–128
- Liang, TG; Huang, XD; Wu, CX; Liu, XY; Li, WL; Guo, ZG; Ren, JZ (2007) 'An application of MODIS data to snow cover monitoring in a pastoral area: A case study in Northern Xinjiang, China.' *Remote Sensing of Environment* 112: 1514–1526
- Li, B; Zhu, A; Zhou, C; Zhang, Y; Pei, T; Qin, C (2008) 'Automatic mapping of snow cover depletion curves using optical remote sensing data under conditions of frequent cloud cover and temporary snow.' *Hydrological Processes* 22: 2930–2942
- Menon, S; Koch, D; Beig, G; Sahu, S; Fasullo, J; Orlikowski, D (2010) 'Black carbon aerosols and the third polar ice cap.' *Atmospheric Chemistry and Physics* 10: 4559–4571
- Miller, SD; Thomas, FL (2005) 'Satellite-based imagery techniques for daytime cloud/snow delineation from MODIS.' *Journal of Applied Meteorology* 44: 987–997
- Mool, PK; Bajracharya, SR; Joshi, SP (2001a) 'Inventory of glaciers, glacial lakes and glacial lake outburst flood monitoring and early warning systems in the Hindu Kush-Himalayan Region – Nepal. Kathmandu, Nepal: ICIMOD
- Mool, PK; Wangda, D; Bajracharya, SR; Kunzang, K; Gurung, DR; Joshi, SP (2001b) *Inventory of glaciers, glacial lakes and glacial lake outburst flood monitoring and early warning systems in the Hindu Kush-Himalayan Region – Bhutan. Kathmandu, Nepal: ICIMOD*
- Negi, HS; Thakur, NK; Kumar, R; Kumar, M. (2009) 'Monitoring and evaluation of seasonal snow cover in Kashmir valley using remote sensing, GIS and ancillary data.' *Journal of Earth System Science* 118: 711–720
- Parajka, J; Blöschl, G (2008) 'The value of MODIS snow cover data in validating and calibrating conceptual hydrologic models.' *Journal of Hydrology* 358(3-4): 240–258
- Pu, Z; Xu, Li (2009) 'MODIS/Terra observed snow cover over the Tibet Plateau: distribution, variation and possible connection with the East Asian Summer Monsoon (EASM).' *Theoretical and Applied Climatology* 97: 265–278
- Rathore, BP; Kulkarni, AV; Sherasia, NK (2009) 'Understanding future changes in snow and glacier melt runoff due to global warming in Wangar Gad basin, India.' *Current Science* 97(7): 1077–1081
- Ramamoorthi, AS; Haefner, H (1991) 'Runoff modelling and forecasting of river basins, and Himalayan snow- cover information system (HIMSIS).' *System* 201: 347–356
- Ramsay, B (1998) 'The interactive multisensory snow and ice mapping system.' *Hydrological Processes* 12: 1537–1546
- Riggs, G; Hall, DK (2002) *Reduction of cloud obscuration in the MODIS snow data product*. Paper presented at the 59th Eastern Snow Conference, 5–7 June 2002, Stowe, Vermont, USA
- Riggs, G; Hall, DK; Salomonson, WV (2006) *MODIS snow products: User guide to collection 5*. Greenbelt MD (USA): NASA/Goddard Space Flight Center. [http://modis-snow-ice.gsfc.nasa.gov/uploads/sug\\_c5.pdf](http://modis-snow-ice.gsfc.nasa.gov/uploads/sug_c5.pdf)
- Robinson, D A; Dewey, KF; Heim, RR (1993) 'Global snow cover monitoring: An update.' *Bulletin of the American Meteorological Society* 74(9): 1689–1696
- Wang, X; Xie, Hongjie (2009) 'New methods for studying the spatiotemporal variation of snow cover based on combination products of MODIS Terra and Aqua.' *Journal of Hydrology* 371: 192–200
- Zhang, Y; Yan, S; Lu, Y (2010) 'Snow cover monitoring using MODIS data in Liaoning Province, Northeastern China.' *Remote Sensing* 2(3): 777–793
- Zurick, D; Pacheco, J; Shrestha, B; Bajracharya, B (2005) *Atlas of the Himalaya*. Kathmandu, Nepal: ICIMOD

# About ICIMOD

The International Centre for Integrated Mountain Development, ICIMOD, is a regional knowledge development and learning centre serving the eight regional member countries of the Hindu Kush-Himalayas – Afghanistan, Bangladesh, Bhutan, China, India, Myanmar, Nepal, and Pakistan – and based in Kathmandu, Nepal. Globalisation and climate change have an increasing influence on the stability of fragile mountain ecosystems and the livelihoods of mountain people. ICIMOD aims to assist mountain people to understand these changes, adapt to them, and make the most of new opportunities, while addressing upstream-downstream issues. We support regional transboundary programmes through partnership with regional partner institutions, facilitate the exchange of experience, and serve as a regional knowledge hub. We strengthen networking among regional and global centres of excellence. Overall, we are working to develop an economically and environmentally sound mountain ecosystem to improve the living standards of mountain populations and to sustain vital ecosystem services for the billions of people living downstream – now, and for the future.





**International Centre for Integrated Mountain Development**

GPO Box 3226, Kathmandu, Nepal

**Tel** +977-1-5003222 **Fax** +977-1-5003299

**Email** [info@icimod.org](mailto:info@icimod.org) **Web** [www.icimod.org](http://www.icimod.org)

ISBN 978 92 9115 218 6